WATER RESOURCES RESEARCH, VOL. 49, 8400–8417, doi:10.1002/2013WR014437, 2013

A stochastic model for high-resolution space-time precipitation simulation

Athanasios Paschalis,[1] Peter Molnar,[1] Simone Fatichi,[1] and Paolo Burlando[1]

Received 16 July 2013; revised 31 October 2013; accepted 4 November 2013; published 16 December 2013.

[1] High-resolution space-time stochastic models for precipitation are crucial for hydrological applications related to flood risk and water resources management. In this study, we present a new stochastic space-time model, STREAP, which is capable of reproducing essential features of the statistical structure of precipitation in space and time for a wide range of scales, and at the same time can be used for continuous simulation. The model is based on a three-stage hierarchical structure that mimics the precipitation formation process. The stages describe the storm arrival process, the temporal evolution of areal mean precipitation intensity and wet area, and the evolution in time of the two-dimensional storm structure. Each stage of the model is based on appropriate stochastic modeling techniques spanning from point processes, multivariate stochastic simulation and random fields. Details of the calibration and simulation procedures in each stage are provided so that they can be easily reproduced. STREAP is applied to a case study in Switzerland using 7 years of high-resolution (2×2 km^2; 5 min) data from weather radars. The model is also compared with a popular parsimonious space-time stochastic model based on point processes (space-time Neyman-Scott) which it outperforms mainly because of a better description of spatial precipitation. The model validation and comparison is based on an extensive evaluation of both areal and point scale statistics at hydrologically relevant temporal scales, focusing mainly on the reproduction of the probability distributions of rainfall intensities, correlation structure, and the reproduction of intermittency and wet spell duration statistics. The results shows that a more accurate description of the space-time structure of precipitation fields in stochastic models such as STREAP does indeed lead to a better performance for properties and at scales which are not used in model calibration.

Citation: Paschalis, A., P. Molnar, S. Fatichi, and P. Burlando (2013), A stochastic model for high-resolution space-time precipitation simulation, *Water Resour. Res.*, *49*, 8400–8417, doi:10.1002/2013WR014437.

1. Introduction

[2] High-resolution space-time precipitation data are essential in many scientific and engineering hydrological applications, in particular those involving rainfall as an input into spatially distributed watershed hydrological models [e.g., *Kollet and Maxwell*, 2008; *Rigon et al*., 2006; *Ivanov et al*., 2004; *Fatichi et al*., 2012a, 2012b, 2013]. Although high-resolution weather radar data may serve this purpose, for risk analysis and design of hydrological systems it is generally better to generate multiple realizations of rainfall fields with a stochastic model and set the problem up in a probabilistic simulation framework [e.g., *Montanari and Koutsoyiannis*, 2012]. The three key elements of a successful stochastic space-time precipitation model are (a) the reproduction of key statistics (intensities, covariance structure, extremes, intermittency) of precipitation at the storm scale, including properties of storm motion; (b) the reproduction of those statistics also on a long-term (continuous) basis, thereby including storm inter-arrival times and other dry period statistics; and (c) model parsimony and tractable parameter estimation procedures. Although many stochastic space-time precipitation modeling approaches exist (see brief review in the next section), we are of the opinion that a single model that satisfies simultaneously and satisfactorily all three requirements does not stand out, and there continues to be a need to develop and test new modeling tools.

[3] In this work, we propose a stochastic precipitation model for the continuous simulation of space-time correlated rainfall fields which reproduces the most important features of the precipitation process as observed from weather radar for a large range of spatial and temporal scales. Although the model is based on established ideas [*Bell*, 1987; *Kundu and Bell*, 2003; *Pegram and Clothier*,

Additional supporting information may be found in the online version of this article.

[1]Institute of Environmental Engineering, ETH Zurich, Zurich, Switzerland.

Corresponding author: A. Paschalis, Institute of Environmental Engineering, ETH Zurich, Wolfgang-Pauli-Str. 15, CH-8093 Zurich, Switzerland. (paschalis@ifu.baug.ethz.ch)

0043-1397/13/10.1002/2013WR014437

2001a], we provide significant improvements to better capture the basic structural features of precipitation such as its intermittent nature, correlation patterns in space and time, positively skewed probability distribution of intensities, and the growth and decay of storms as well as their movement (advection). We provide the analytical basis for the model and we demonstrate its performance for a range of hydrologically relevant statistics.

[4] We are of the opinion that the requirement of model parsimony and especially a coherent estimation procedure are very important for applications. Therefore, one of the key contributions of this paper is to provide a detailed framework for model calibration, which can make the model widely applicable for studies of basin hydrological response, flood risk, urban drainage design, etc. The scales of applications we are targeting reflect those of the highest resolutions available from observations, i.e., ground-based precipitation monitoring networks (rain gauges) with $\sim$10 min resolution and technologically advanced weighing and optical sensors, as well as remote sensing of spatial precipitation (weather radar, satellite) at $\sim$1 km^2 resolution. The latter are only widely available in the last decades [e.g., *Kummerow et al*., 1998; *Berne and Krajewski*, 2012].

[5] This paper is structured as follows. We first provide a brief review of space-time modeling of precipitation in section 2. This is followed by a detailed description of the new model STREAP in section 3 and its calibration in section 4. The data for the application are provided in section 6 and finally the results are presented in section 7 for areal and point-scale statistics separately. The performance of the new model is also compared with a benchmark; a widely used version of the space-time Neyman-Scott, which is described briefly in section 5. We close the article with some considerations for further improvements and conclusions.

2. A Brief Review of Space-Time Modeling

[6] The existing stochastic spatiotemporal modeling approaches can be divided into four major groups. The approach of the first group is to simplify the problem of spatiotemporal modeling into a multisite temporal simulation framework [*Wilks*, 1998; *Brissette et al*., 2007; *Wilks*, 1999; *Kleiber et al*., 2012; *Bárdossy and Pegram*, 2009]. This approach is very appealing when only point-scale measurements are available. Existing models exploit stochastic processes spanning from multivariate chain-dependent processes [e.g., *Wilks*, 1998] to copula-based approaches [*Bárdossy and Pegram*, 2009] and hidden Markov processes [*Hughes et al*., 1999]. In general, since these models focus mainly on the stochastic simulation of precipitation in time at specific locations, their representation of the spatial distribution of precipitation is poor. Moreover, they are generally applied at a daily time step which is not adequate for high-resolution applications.

[7] The second approach is based on the theory of point processes and is a generalization of the ideas that were first introduced for rainfall modeling in time. These models have become some of the most widely used and robust tools for precipitation simulation [e.g., *Burton et al*., 2008, 2010; *Leonard et al*., 2008; *Cowpertwait et al*., 2002; *Beuchat et al*., 2011; *Cowpertwait*, 2010]. The common aspect is that rainfall patterns in space are simulated as a superposition of two-dimensional pulses (rain cells). The simplest, yet most widely used approach is to assume the shape of the cells to be discs with a uniform or Gaussian-distributed intensity during their lifetime, and their occurrence in space and time to be a Poisson process [e.g., *Cowpertwait et al*., 2002; *Féral et al*., 2006; *Burton et al*., 2008]. Under this assumption the analytical derivation of the statistical properties across scales is possible. More complex approaches include the WGR (Waymire - Gupta - Rodriguez Iturbe) model [*Waymire et al*., 1984] which reproduces more realistic precipitation patterns including anisotropy, advection, etc., and the modified turning bands model [*Mellor*, 1996; *Mellor and O'Connell*, 1996]. Key problems with space-time point process model applications are their poor performance in capturing complex spatial structure, kinematic properties of rain cells, and a general overparameterization which may lead to a difficult calibration.

[8] The third approach is based on the theory of random fields. Generally, these models have been developed to fill the gap in space-time precipitation simulation at high-resolution scales (typically $\sim$1 km^2, $\sim$5 min). They typically simulate precipitation as a nonlinear transformation of two-dimensional or three-dimensional Gaussian random fields adopting some parametric form for their covariance [e.g., *Pegram and Clothier*, 2001b; *Bell*, 1987; *Durbán and Glasbey*, 2001; *Kumar and Bell*, 2006; *De Michele and Bernardara*, 2005; *Koutsoyiannis et al*., 2011]. The most popular representations of the spatial structure at the mesoscale includes models with covariances of the exponential type [*Bell*, 1987], fractional Gaussian noise [*Koutsoyiannis*, 2011], and fractional Brownian motion [*Pegram and Clothier*, 2001a]. This group of models has been mostly used for event-based simulation and few attempts have been directed at continuous simulation.

[9] The fourth approach is based on theories of scale invariance, and especially on the use of two-dimensional or three-dimensional multifractal processes for rainfall simulation. The attractive feature of such an approach is that statistics across spatiotemporal scales are explicitly linked in a parsimonious manner. Multiplicative random cascade models which simulate the cascade of rainfall depth across scales by independent multipliers are typically used for simulation [e.g., *Over*, 1995; *Schertzer and Lovejoy*, 1987]. It has been found that this simulation framework leads to a satisfactory representation of several key aspects of precipitation (e.g., the power law distribution of extremes), and for this reason it became a very popular tool for rainfall stochastic simulation [e.g., *Over and Gupta*, 1996; *Deidda*, 2000; *Gires et al*., 2012; *Kang and Ramírez*, 2010; *Menabde et al*., 1997; *Pathirana and Herath*, 2002]. One of the main practical constraints of this approach is that the traditional discrete simulation procedure of the multiplicative random cascades generates very unrealistic blocky patterns in space [*Kang and Ramírez*, 2010]. Continuous simulation algorithms have been developed as well [*Pecknold et al*., 1993], however, with fewer applications reported in the literature.

3. Formulation of STREAP

[10] In this section, we provide the mathematical formulation of the constitutive blocks of a new space-time

stochastic precipitation model. The model is named STREAP as an abbreviation of Space-Time Realizations of Areal Precipitation. The structure of the model is a substantial improvement of the previous works of *Bell* [1987], *Kundu and Bell* [2003], and mainly *Pegram and Clothier* [2001a]. The model adopts well established ideas developed in the analysis of time series and random fields spanning from point processes to multidimensional random fields.

[11] The main idea of STREAP is that space-time precipitation can be considered as a realization of a stochastic process that consists of various subprocesses, each one describing a fundamental structural feature of precipitation. The structure of the STREAP model is based on a three-stage hierarchical basis identical to *Clothier and Pegram* [2002]. The three stages are: (1) storm arrival process; (2) process describing the within-storm temporal evolution of areal precipitation properties; and (3) process describing the temporal evolution of the two-dimensional storm structure. This structure, schematically illustrated in Figure 1, is key to the application of the model because it separates different processes in an explicit manner and draws clear connections with the natural phenomenology of precipitation at each stage.

3.1. Storm Arrival Process

[12] The storm arrival process is represented using an alternating renewal process describing a temporal sequence of dry and wet periods in the region of interest [e.g., *Bernardara et al*., 2007; *Ng and Panu*, 2010; *Veneziano*, 2002; *Roldan and Woolhiser*, 1982; *Menabde and Sivapalan*, 2000; *Pegram and Clothier*, 2001b]. The dry and wet spell durations are sampled from specific probability distributions and are mutually independent. The probability distribution of the wet spell duration is assumed to be a generalized Pareto [e.g., *Embrechts et al*., 1997] with parameters $k_{\text{wet}}, \sigma_{\text{wet}}, \theta_{\text{wet}}$. The dry spell duration is assumed to follow a lognormal distribution [e.g., *Papoulis and Unnikrishna*, 2002] with parameters $\mu_{\text{dry}}, \sigma_{\text{dry}}$.

[13] For each wet period, an average wind speed and direction have also to be defined. Our preliminary data analysis showed that wind speed is well described by a two parameter gamma distribution [*Papoulis and Unnikrishna*, 2002] with parameters $\alpha_{\text{wind}}, \beta_{\text{wind}}$; and for wind direction, we suggest to use the empirical probability density function (pdf) because it is very unlikely that a given parametric pdf will fit well the bounded [0–360°] distribution of wind direction.

[14] The selection of the above probability distributions has no physical meaning and is simply based on a good fit to the data of storm arrival for a given region (see section 6). Different distributions can be used if they are found to fit storm data better, without undermining the model concept and structure.

3.2. Temporal Evolution of Mean Areal Statistics

[15] In the second stage of the model, the simulation of the mean areal statistics of the precipitation field is performed. The two random variables that describe the development of the storm are the fraction of the wet area and the mean areal precipitation intensity in the simulated domain. These two random variables are abbreviated hereafter as WAR and IMF following the notation of *Pegram and Clothier* [2001a]. The two variables are autocorrelated and cross correlated and thus have to be simulated as a bivariate stochastic process.

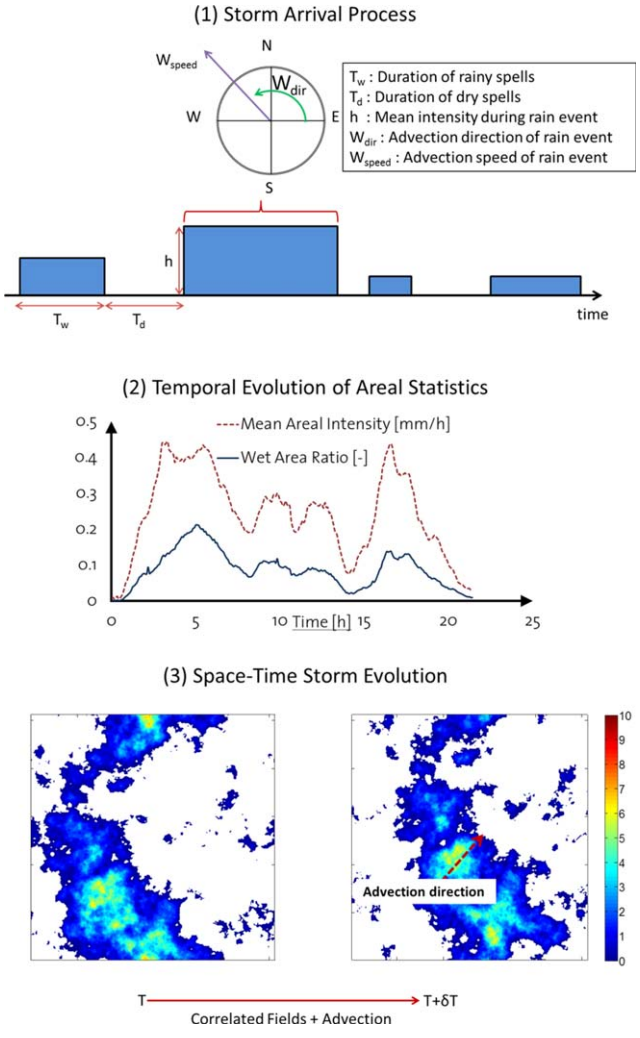

Figure 1. Schematic representation of the STREAP model.

3.2.1. The Bivariate WAR-IMF Process

[16] The variables of interest (WAR, IMF) are simulated as a probability transformation of the Gaussian processes WAR_g, IMF_g. For each storm, we define the bivariate processes $\text{WAR}_g \sim N(\mu_W, \sigma_W)$ and $\text{IMF}_g \sim N(\mu_I, \sigma_I)$ as Gaussian stochastic processes with a covariance function belonging to the Whittle-Matérn class, which is one of the most widely used parametric forms in geostatistics due to its generality and flexibility [e.g., *Gneiting*, 2010; *Hristopulos and Elogne*, 2009; *Storvik et al*., 2002; *Christakos*, 1987; *Guttorp and Gneiting*, 2006].

[17] The autocovariance and cross-covariance functions of each process are defined respectively as [*Gneiting*, 2010]:

$$R_W(h) = \sigma_W^2 M(h|\nu_W, \alpha_W), \quad (1)$$

$$R_I(h) = \sigma_I^2 M(h|\nu_I, \alpha_I), \quad (2)$$

$$R_{WI}(h) = R_{IW}(h) = \rho_{WI}\sigma_W\sigma_I M(h|\nu_{WI}, \alpha_{WI}), \quad (3)$$

where the subscripts W and I refer to the WAR_g and IMF_g processes respectively, ρ_{WI} is the cross-correlation

coefficient, h is the lag time for a temporal stochastic process, σ_I and σ_W are the standard deviations of WAR_g and IMF_g, and $M(h|v,\alpha)$ is defined as [*Gneiting*, 2010]:

$$M(h|v,\alpha)=\frac{2^{1-v}}{\Gamma(v)}(\alpha|h|)^{v}K_v(\alpha|h|), \quad (4)$$

where $K_v(\alpha|h|)$ is the modified Bessel function of the second kind. The bivariate process is stationary and thus the covariances are only dependent on the lag h and on the parameters of the covariance function.

[18] We further assume that the auto/cross correlation of the WAR_g-IMF_g process is unique for all the storms on a seasonal basis. In other words, the parameters that define the autocorrelation and cross-correlation $\alpha_W, \alpha_I, v_W, v_I, \alpha_{WI}, v_{WI}, \rho_{WI}$ remain invariant for all the storms in one season.

[19] The parameters $\mu_w, \mu_I, \sigma_W, \sigma_I$ that define the mean values and the standard deviations of the WAR_g-IMF_g process per each storm are correlated to each other and also with the storm duration T_w. We model the relationships among the five parameters with a multidimensional copula. The marginals of $\mu_w, \mu_I, \sigma_W, \sigma_I$ are approximated as Gaussian and T_w follows a generalized Pareto distribution as explained in section 3.1. A copula function for n random variables $X_1, X_2, \ldots, X_n$ can be defined as

$$C(u_1,u_2,\ldots,u_n)=P[U_1\le u_1, U_2\le u_2,\ldots,U_n\le u_n], \quad (5)$$

where $U=F(X)$ is the cumulative distribution function. We used the parametric form of the multivariate T-copula with parameters P_c, v_c [e.g., *Demarta and McNeil*, 2007].

[20] Finally, WAR_g(t) and IMF_g(t) are transformed to WAR(t) and IMF(t), respectively, according to a distribution anamorphosis scheme [*Schleiss et al*., 2012] which is defined as

$$\mathrm{WAR}(t)=F^{-1}[U(\mathrm{WAR}_g(t))], \quad (6)$$

$$\mathrm{IMF}(t)=F^{-1}[U(\mathrm{IMF}_g(t))], \quad (7)$$

where U is the quantile function and F^{-1} is the inverse cumulative probability distribution function which demands for a definition of the marginal distributions of WAR and IMF. Being bounded (between 0 and 1), WAR follows a Beta distribution [*Papoulis and Unnikrishna*, 2002] with parameters α_b, β_b, and IMF a two parameter Gamma distribution with parameters α_γ, b_γ.

[21] The parametric forms adopted both for the copula and the distributions of WAR(t) and IMF(t) were chosen due to the good fit they provided for the data used in this study (section 6). There is no other physical consideration behind those choices and users may decide on different distributions which better fit their datasets, also in this case without compromising the model structure and concept.

3.2.2. Modeling of the Bivariate WAR-IMF Process

[22] Since the computation speed of a stochastic model is an important aspect, we chose to model the Gaussian bivariate process WAR_g-IMF_g in the frequency domain, exploiting fast computation algorithms of the Fast Fourier Transform (FFT). The details of this procedure can be found in *Chambers* [1995]. The only requirement is the derivation of the spectral and cross-spectral densities corresponding to the Whittle-Matérn covariance. The spectral densities are the Fourier transforms of the covariance functions and thus [*Chorti and Hristopulos*, 2008]:

$$S(k)=\mathcal{F}[cM(h|v,\alpha)]=c\frac{\Gamma(v+\frac{1}{2})\alpha^{2v}}{\Gamma(v)\pi^{\frac{1}{2}}}\frac{1}{(\alpha^2+k^2)^{v+\frac{1}{2}}}, \quad (8)$$

where $c\in\Re$, k is the wave number, and $\mathcal{F}[.]$ is the one-dimensional Fourier transform.

[23] In brief, the algorithm used to simulate the WAR_g-IMF_g is as follows:

1. For each storm, we estimate the spectral and cross-spectral densities according to equation (8). The spectral density of WAR_g is estimated for $v=v_W, \alpha=\alpha_W$ and $c=f(\sigma_W^2)$, the spectral density of IMF_g is estimated for $v=v_I, \alpha=\alpha_I$ and $c=f(\sigma_I^2)$, and the cross-spectral density is estimated for $v=v_{WI}, \alpha=\alpha_{WI}$ and $c=f(\sigma_W,\sigma_I,\rho_{WI})$;
2. Having estimated the spectral and cross-spectral densities, we can generate the Fourier coefficients of WAR_g-IMF_g [*Chambers*, 1995];
3. Finally, WAR_g-IMF_g are obtained by taking the inverse Fourier transform of these coefficients.

3.3. Spatiotemporal Evolution of the Storm Structure

[24] From the previous two simulation steps, the fraction of the wet area WAR(t) and the precipitation intensity IMF(t) over the domain are known for every time step. In the third stage of the STREAP model, this information is transformed into the space-time evolution of the precipitation fields.

3.3.1. Spatial Precipitation Fields

[25] Precipitation fields in space are modeled as latent Gaussian fields [e.g., *Kleiber et al*., 2012; *De Oliveira*, 2004; *Durbán and Glasbey*, 2001]. Let $G(x,y)$ be an isotropic, stationary two-dimensional normally distributed $\sim N(0,1)$ random field with spatial autocorrelation function $\rho_g[(x,y),(x+s_x,y+s_y)]$. Since $G(x,y)$ is assumed to be wide sense stationary and isotropic, then the autocorrelation depends only on the distance $s=\sqrt{s_x^2+s_y^2}$. The simplest one-parameter exponential autocorrelation function is adopted here similarly to *Bell* [1987]. Its parametric form is

$$\rho_g(s)=\exp(-\frac{s}{\alpha_g}), \quad (9)$$

where α_g is the correlation length. Different assumptions concerning the spatial autocovariance function have been adopted in previous studies. For example, *Pegram and Clothier* [2001b] adopted a nonstationary two-dimensional fractional Brownian motion (FBM) while *Mandapaka et al*. [2009] adopted a two-parameter exponential autocorrelation function. Here for the sake of parsimony we use the simplest possible form (equation (9)) which is also well supported by data [*Paschalis*, 2013]. Then the intermittent precipitation fields can be expressed as:

$$R(x,y,t)=\begin{cases} 0 & , \quad \text{for } U[G(x,y,t)] < \text{1-WAR}\ (t), \\ LN^{-1}\left(\dfrac{U[G(x,y,t)]-1+\text{WAR}\ (t)}{\text{WAR}\ (t)}, \mu_r, \sigma_r\right) & , \quad \text{for } U[G(x,y,t)] \geq \text{1-WAR}\ (t), \end{cases} \tag{10}$$

where $R(x,y,t)$ is the rainfall intensity in space and time, LN^{-1} is the inverse cumulative lognormal distribution, and μ_R, σ_R are the parameters of the lognormal distribution.

[26] For the sake of parsimony, we further assume that the coefficient of variation of the positive part of the distribution of the spatial fields, CV_r, is only dependent on the month and is the same for all storms. Once the mean intensity IMF(t), the fraction of wet area WAR(t) and the coefficient of variation of the positive part of the distribution of spatial rainfall are known, the estimation of the parameters of the lognormal distribution μ_r, σ_r needed for (10) is achieved by solving the system of equations for the first and second-order moments of the lognormal distribution.

[27] Note that the autocorrelation of the transformed fields $R(x,y)$ is different from the Gaussian case $G(x,y)$. The autocorrelation of the transformed fields does not have an analytical expression and can only be approximated numerically [e.g., *Guillot*, 1999].

3.3.2. Temporal Evolution of the Precipitation Fields

[28] The spatial precipitation fields are correlated in time. This correlation is introduced in the STREAP model by assuming the following autoregressive moving average ARMA(p,q) representation for the Gaussian fields.

$$G(x,y,t)=\sum_{i=1}^{p}\phi_i G(x,y,t-i)+\sum_{j=1}^{q}\theta_j \epsilon(x,y,t-j)+\epsilon(x,y,t), \tag{11}$$

where the noise term $\epsilon(x,y,t)$ is a Gaussian two-dimensional random field with the same spatial autocorrelation as $G(x,y,t)$. The variance of the noise term is estimated from the unit variance restriction of the field $G(x,y,t)$ [*Box and Jekins*, 1970].

[29] The temporal evolution of the field refers to the Lagrangian system of coordinates, i.e., following the field motion. In this study, we use an ARMA(2,2) model because of a good fit to our data, but this result would be difficult to generalize, and different orders could eventually be used in other applications [e.g., *Clothier and Pegram*, 2002; *Bell and Kundu*, 1996; *Kundu and Bell*, 2003]. In this study, the parameters of the ARMA model are held constant for the entire simulation period, due to the strong uncertainties involved in their estimation.

3.3.3. Modeling of the 2-D Gaussian Fields

[30] We simulate the two-dimensional fields by 2-D FFTs [*Lang and Potthoff*, 2011]. This means that G can be defined as:

$$G(x,y)=(\mathcal{F}^{-1}S^{1/2}\mathcal{F}Z)(x,y). \quad x,y\in\Re, \tag{12}$$

where S is the two-dimensional power spectrum, Z is a two-dimensional Gaussian noise and $\mathcal{F}^{-1}$ is the inverse Fourier transform. In order to simulate Gaussian random fields with an exponential decay of the autocorrelation, the 2-D spectrum $S(k_x,k_y)$ has to be calculated,

$$S(k_x,k_y)=\mathcal{F}\left[\sigma^2\exp\left(-\frac{|(s_x,s_y)|}{\alpha_g}\right)\right], \quad k_x,k_y,s_x,s_y\in\Re, \tag{13}$$

where σ^2 is the variance of the Gaussian field $G(x,y)$, which in this case $\sigma^2=1$. Since the autocovariance function is symmetric, the two-dimensional Fourier transform of (13) can be reduced to the one-dimensional Hankel transform [*Bracewell*, 2000, pp. 336],

$$S(|k|)=2\pi\int_0^\infty \sigma^2\exp\left(-\frac{s}{\alpha_g}\right)J_0(2\pi|k|s)s \quad \mathrm{d}s = \sigma^2\frac{2\pi\frac{1}{\alpha_g}}{\left(4\pi^2|k|^2+(\frac{1}{\alpha_g})^2\right)^{\frac{3}{2}}}, \tag{14}$$

where k_x, k_y are the wave numbers for the two spatial dimensions, $|k|=\sqrt{k_x^2+k_y^2}$, and J_0 is the Bessel function of the first kind of order zero.

[31] Importantly, the ARMA representation of the Gaussian field as defined in (11) can be expressed with an equivalent ARMA representation of the Fourier coefficients of the Gaussian random field for each time step t, $W_G=\mathcal{F}Z(k_x,k_y,t)$, as:

$$\mathcal{F}Z(k_x,k_y,t)=W_G(k_x,k_y,t)=\sum_{i=1}^{p}\phi_i W_G(k_x,k_y,t-i) +\sum_{j=1}^{q}\theta_j\epsilon_W(k_x,k_y,t-j)+\epsilon_W(k_x,k_y,t), \tag{15}$$

where $\epsilon_W(k_x,k_y,t)$ is an uncorrelated Hermitian white noise Gaussian complex random field. This can be shown by multiplying (15) element by element with the square root of the power spectral density $S(k_x,k_y)^{1/2}$ and taking the 2-D inverse Fourier transforms considering equation (12). The relationship (15) gives the direct way of simulating the space-time Gaussian fields in Lagrangian coordinates.

[32] *Kundu and Bell* [2003] and *Bell* [1987] stated that for precipitation, low-frequency components should have higher correlation than high-frequency ones. Conceptually this means that large-scale features (e.g., fronts) are more correlated than small-scale fluctuations (e.g., rain cells). Even though this feature would perhaps increase the realism of the model, it would also prohibitively complicate its calibration.

[33] The generated fields, due to the symmetries of the fast Fourier transform, can be folded. This property can be

Table 1. Input for the STREAP Model

Parameters of the STREAP Model		Estimated From
First stage		
$\kappa_{wet}, \sigma_{wet}, \theta_{wet}$	Parameters of the generalized Pareto distribution of the wet spells	WAR series
μ_{dry}, σ_{dry}	Parameters of the lognormal distribution of dry spells	WAR series
$\alpha_{wind}, \beta_{wind}$	Parameters of the Gamma distribution of wind speed	Radar data by a correlation matching algorithm
Empirical distribution	Distribution of the wind directions	Radar data by a correlation matching algorithm
Second stage		
$\alpha_W, \alpha_I, \nu_W, \nu_I, \alpha_{WI}, \nu_{WI}, \rho_{WI}$	Parameters of the Whittle-Matern Covariance function	Normalized WAR,IMF series
P_c, ν_c	Parameters of the T-copula	Normalized WAR,IMF series and storm duration
α_b, β_b	Parameters of the Beta distribution of WAR	WAR series
$\alpha_\gamma, \beta_\gamma$	Parameters of the Gamma distribution of IMF	IMF series
Third stage		
α_g	Spatial correlation length	Radar images
CV_r	Coefficient of variation of spatial precipitation	Radar images
ϕ_i, θ_i	Parameters of the ARMA process	Radar images

exploited to simulate advection of the fields in the Eulerian coordinate system. In STREAP, in order to avoid artifacts due to field symmetries, we suggest to simulate precipitation fields for a larger spatial extent and then use only the central area of the simulations as the model output. This procedure was also used by in the original model by *Pegram and Clothier* [2001a] and *Clothier and Pegram* [2002].

4. Model Calibration

[34] A well-defined calibration of the STREAP model is essential for applications. High-resolution weather radar data are required for the calibration, which is done through a series of steps that lead to a robust parameter estimation.

[35] One of the main disadvantages of STREAP is that analytical derivation of the statistical properties of the simulated fields is mathematically intractable, differently from the Poisson cluster models [e.g., *Burton et al*., 2008; *Cowpertwait*, 2010; *Burton et al*., 2010], which have analytical expressions for their moments and covariance functions. These expressions can be used for a direct and straightforward parameter estimation. This is not possible with the model developed here and each stage shown in Figure 1 is calibrated separately. In order to capture the seasonality of precipitation, most of the processes should be calibrated on a seasonal basis (some even on a monthly basis), as described below.

4.1. Storm Arrival Process

[36] This stage is the most straightforward to calibrate. Parameters of the distribution of the durations of the dry and wet periods are extracted and estimated from the data by the maximum likelihood method. Although the fitting procedure is clear, the difficulty lies in the separation of precipitation events [e.g., *Veneziano and Lepore*, 2012; *Koutsoyiannis and Foufoula-Georgiou*, 1993; *Lakshmanan et al*., 2003]. First, we define the study area and then the sequence of WAR(t) is extracted from the radar data. In order to smooth the signal, a moving average filter with a 1 h window is applied to the sequence. The precipitation event (storm) is defined as the time when the filtered time series of WAR(t) exceeds a low (2%) threshold. If the time between two storms is less than 2 h then those events are considered to consist of one storm structure. It should be noted that this storm event definition reflects persistence in the rain-covered area in the selected region and is generally much longer than the typical point-scale storm duration estimated from rain gauges. The parameters estimated at this step are $\kappa_{wet}, \sigma_{wet}, \theta_{wet}, \mu_{dry}, \sigma_{dry}$ (Table 1).

4.2. Storm Advection

[37] For each of the identified storm events from the previous step, the storm speed is estimated using a correlation matching algorithm. From the radar image sequence during an event we calculate the spatial displacements that maximize the correlation for two consecutive images ($\delta x(t)$ (km), $\delta y(t)$ (km)). Repeating this procedure for the entire event, we construct the "storm path." From this path, we estimate the average velocity of the event as $U_{storm} = \left(\left(\sum_{t=0}^{t=T_W} \delta x(t) \right)^2 + \left(\sum_{t=0}^{t=T_W} \delta y(t) \right)^2 \right)^{0.5} / T_W$, where T_W is the storm duration.

[38] Subsequently, the parameters $\alpha_{\text{wind}}, \beta_{\text{wind}}$ of the Gamma distribution for the wind speed (Table 1) are estimated using maximum likelihood. Although this velocity can only be considered as an approximation of the true storm speed, we consider this adequate for the purposes of the calibration of the stochastic model.

4.3. Temporal Evolution of Mean Areal Statistics

[39] The calibration of the WAR-IMF process has several components. First the parameters of the Whittle Matern function have to be estimated. To this end, the estimated sequences of WAR(t)-IMF(t) derived from the radar data are normalized, i.e.,

$$\text{WAR}_g(t) = N^{-1}(U(\text{WAR}(t)), 0, 1), \quad (16)$$

$$\text{IMF}_g(t) = N^{-1}(U(\text{IMF}(t)), 0, 1). \quad (17)$$

[40] Then the sample autocorrelation and cross correlations are estimated and, finally, the parameter estimation is conducted by constrained least squares fitting of the theoretical parametric functions. The constraint arises from the restriction that the covariance has to be positive definite [*Gneiting*, 2010]. Alternatively, a maximum likelihood estimation can be used as well. This step results in the

estimation of the parameters $\alpha_W, \alpha_I, v_W, v_I, \alpha_{WI}, v_{WI}, \rho_{WI}$ (Table 1).

[41] In order to obtain the mean values and standard deviations of the Gaussian processes WAR$_g(t)$-IMF$_g(t)$ for each storm, the parameters of the copula have to be estimated. This is done by calculating from each storm the mean values and standard deviations of the normalized sequences of WAR and IMF ($\mu_W, \mu_I, \sigma_W, \sigma_I$). These values are then used in the fitting of the five-dimensional copula using approximate maximum likelihood for the quantities $U(\mu_W), U(\mu_I), U(\sigma_W), U(\sigma_I), U(T_W)$. The fitting to the marginals of $\mu_W, \mu_I, \sigma_W, \sigma_I, T_W$ is done by maximizing their respective likelihood functions. This procedure leads to the estimation of the parameters P_c, v_c of the T-copula (Table 1). The parameters of the Beta and Gamma distributions $\alpha_b, \beta_b, \alpha_\gamma, \beta_\gamma$ are estimated directly from WAR(t) and IMF(t) series respectively (Table 1).

4.4. Spatial Precipitation Fields

[42] A direct estimation of the spatial autocorrelation function can be highly problematic due to noise corruption and clutter contamination of the radar data and because an analytical expression for autocorrelation of the lognormally distributed intermittent fields cannot be derived. For these reasons, the parameter estimation of the autocorrelation function is conducted only on the binary [0–1] rain-no rain process, which is expected to be well represented by the radar data and relatively free of errors. The methodology followed here is similar to that presented by *Gutnisky and Josić* [2010].

[43] The spatial autocovariance of the binary rain-no rain process above a threshold h, $C_b(s)$, of a latent Gaussian field is related to its autocovariance, $C_g(s)$, as [*Gutnisky and Josić*, 2010]:

$$C_b(s) = p(s) - r^2, \tag{18}$$

where

$$p(s) = \int_h^\infty \int_h^\infty \frac{1}{2\pi\sqrt{1-C_g(s)^2}} \exp\left\{-\frac{a^2+b^2-2C_g(s)ab}{2[1-C_g(s)^2]}\right\} \mathrm{d}a\,\mathrm{d}b, \tag{19}$$

and

$$r = \frac{1}{\sqrt{2\pi C_g(0)}} \int_h^\infty \exp\left(-\frac{y^2}{2C_g(0)}\right) \mathrm{d}y. \tag{20}$$

[44] The parameter α_g is then estimated with ordinary least square fitting of the theoretical spatial covariance function $C_g(s) = \exp(-s/\alpha_g)$. The estimation of $C_g(s)$ from $C_b(s)$ is achieved by a numerical solution of (19) and (20).

[45] For simplicity, the parameter α_g is considered constant on a seasonal basis and equal to the mean value of the estimated $\alpha_g(i)$, where i stands for the i-th temporal step, from the radar images. For each month the spatial coefficient of variation, CV$_r$, is also estimated from the radar images (Table 1).

4.5. Temporal Evolution of the Precipitation Fields

[46] The most difficult and uncertain task in the calibration of STREAP is the estimation of the parameters of the ARMA model, i.e., the temporal evolution of the precipitation fields in the Lagrangian coordinates. In their first presentation of the String of Beads model (SBM), *Pegram and Clothier* [2001a] did not provide a calibration algorithm for this stage and used a "trial and error" procedure to find a parameter set suitable for their data. Here, we propose to estimate the average autocorrelation function of the normalized precipitation fields in time in Lagrangian coordinates and use a constrained least squares fitting procedure of the theoretical autocorrelation function of the ARMA process to the data. The constraint arises from the stability criteria of the ARMA process [*Box and Jekins*, 1970].

[47] The major issue is to identify the Lagrangian coordinate system from the data because observed precipitation fields are only approximately advected with a constant velocity and are subject to rotation and differential velocities. For this reason, we apply a selection criterion in order to restrict the calibration only for storms with negligible differential movement and rotation. In order to identify storms that are moving approximately constantly, we use the storm tracking algorithm COTREC (Continuity of TREC (Tracking Radar Echoes by Correlation)) [*Rinehart and Garvey*, 1978; *Li et al*., 1995]. The method is based on correlation matching imposing a mass conservation (continuity) restriction. Using such a tracking procedure the two-dimensional velocity fields can be estimated for every radar image sequence. Then, the temporal autocorrelation function is estimated from selected storms that fulfill several criteria. In order to exclude events with strong differential movement, a threshold selection is implemented on the mean value of the standard deviation of the spatial velocity vectors estimated using COTREC. A similar criterion is applied on the standard deviation of the advection directions. Finally, we exclude short storms by choosing only those that exceed a specific duration (>3 h). This procedure leads to the parameters ϕ_i, θ_j of the ARMA model, which are considered constant for the entire simulation period. Even though seasonal differences are expected, due to the large uncertainty of the estimation of those parameters, we chose to keep them invariant.

5. Model Benchmark: The Neyman-Scott Space-Time Model

[48] In order to judge the performance of the STREAP model, we benchmark its performance with a simpler and widely used model for precipitation, the Neyman-Scott space-time model, NS(s-t). This model [*Burton et al*., 2008, 2010; *Cowpertwait*, 2006; *Cowpertwait et al*., 2002] is based on point processes theory and simulates rainfall as a superposition of circular rain cells that have a constant intensity during their lifespan. The mathematical formulation of the model and its calibration procedures can be found in *Cowpertwait et al*. [2002]. In summary, NS(s-t) is structured as follows:

1. Storms arrive as a Poisson process in time with rate $\lambda(\mathrm{h}^{-1})$.
2. Each storm origin is followed by a generation of $N(N \geq 0)$ rain cells that form a two-dimensional homogeneous Poisson process with density $\phi_c(\mathrm{km}^{-2})$.
3. The time between the storm origin and the cell arrival is exponentially distributed with parameter $\beta_c(\mathrm{h}^{-1})$.

4. The lifetime of a rain cell follows an exponential distribution with parameter $\eta(\mathrm{h}^{-1})$.
5. The rain cells have uniform intensity during their lifetime which is distributed according to a Weibull distribution with parameters α_c and θ_c.
6. The rain cells are circular and their diameter is exponentially distributed with parameter $\varphi(\mathrm{km}^{-1})$.

[49] This model has been previously found to provide good results and has been successfully applied in different climate types such as Oceanic [*Cowpertwait*, 2006], Mediterranean [*Cowpertwait et al*., 2002], and even in areas with considerable orographic influences on the precipitation distribution [*Bordoy*, 2013]. The model is just one of the existing versions of the Neyman-Scott space-time models. Recently, new developments have been suggested in order to improve the model efficiency for high temporal resolutions and take into account spatial heterogeneity of rainfall [e.g., *Cowpertwait*, 2010; *Burton et al*., 2010].

[50] The calibration procedure of the NS(s-t) model is based on the generalized method of moments as presented by *Burton et al*. [2010]. The statistics we selected for parameter estimation are the mean, standard deviation, coefficient of skewness, probability of no rainfall, and the cross correlation between stations for the aggregation intervals of 1 h and 1 day. The model is calibrated with point-scale (rain gauge) measurements over the study region.

6. Data and Study Area

[51] The study area that was selected to calibrate and validate the STREAP model is shown in Figure 2. This area is located on the Mediterranean side of the European Alps and roughly corresponds to the area examined during the Mesoscale Alpine Program (MAP), [*Bougeault et al*., 2001; *Rotunno and Houze*, 2007; *Buzzi and Foschini*, 2000; *Houze et al*., 2001]. The precipitation climatology of this area has several important distinct features [e.g., *Frei and Schär*, 1998; *Molnar and Burlando*, 2008; *Paschalis et al*., 2012].

[52] The orography that highly influences precipitation generation is the main divide of the European Alps (Figure 2a). Its high altitudes and its bow shape influence precipitation generation due to orographic uplifting and air blocking mechanisms [e.g., *Panziera and Germann*, 2010; *Houze et al*., 2001]. Precipitation in this area is connected with the wet anomaly located around the Lake Maggiore (Figure 2b). The main source of moisture comes from the Mediterranean sea. Intense convective events with strong orographic enhancement occur during the warm seasons (Spring-Summer). These events lead to high precipitation accumulations and high intensities. During summer the effect of the diurnal cycle is also present and intense storms usually take place in the afternoon by convection [*Houze*, 2012]. During winter, storms are mostly stratiform and driven by frontal systems, which leads to low precipitation accumulations.

[53] The study area is well monitored by rain gauges (Figure 2a) and covered by the operational weather radars of the Federal Office of Meteorology and Climatology (MeteoSwiss). In this study, we use both rain gauge and radar measurements. The rain gauges are part of the SwissMetNet monitoring network and are heated tipping-bucket instruments with temporal resolution of 10 min and a tip volume of 0.1 mm. The data are considered very reliable and have been analyzed extensively in previous studies [*Molnar and Burlando*, 2008; *Beuchat et al*., 2011; *Paschalis et al*., 2012]. Rain gauge measurements used in this study extend from 1981 to 2009. Point-scale measurements were not used for the calibration and validation of the STREAP model but only for the space-time Neyman-Scott model.

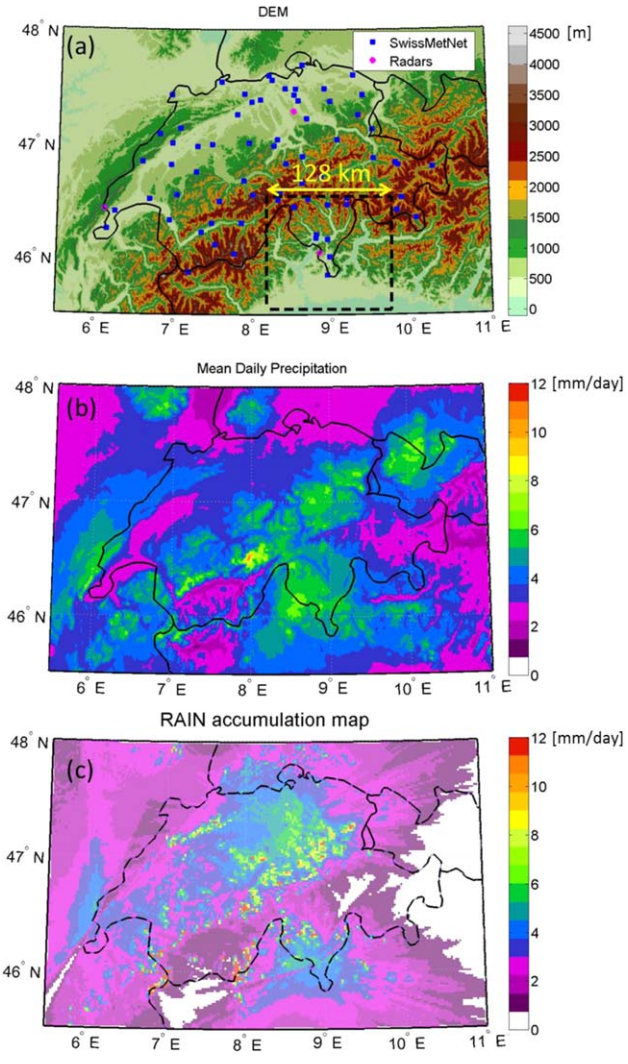

Figure 2. (a) The digital elevation model (DEM) of the area. The box marked with a dashed line highlights the study area. (b) The long-term precipitation (1951–2010) climatology of the area after *Frei and Schär* [1998]. (c) The precipitation climatology as measured from the operational weather radars of MeteoSwiss.

[54] The data from the operational weather radars of MeteoSwiss are used for the calibration and validation of the STREAP model. The product used is the best estimate of precipitation at the ground (RAIN) [*Germann et al*., 2006] and is a composite of the three operational C-band single polarization Doppler radars operated by MeteoSwiss. The temporal resolution of the records is 5 min and the spatial resolution 2×2 km^2. The radar intensities are binned into 16 lognormally distributed classes [*Savina et al*., 2012]. The data extend from 2004 to 2010.

[55] Many problems in precipitation quantification using weather radars exist in orographically complex areas, e.g., strong clutter, beam shielding, low coverage of the vertical sampling volume, etc. These problems can lead to errors in the quantification of precipitation amount (Figure 2c, *Paschalis* [2013]). However, for the area examined here, the problems concerning beam shielding are minor and the radars have good visibility of the vertical profile [*Germann et al*., 2006; *Foresti et al*., 2012]. The only remaining issue in this area is the signal attenuation with distance from the Monte Lema radar, especially toward the South, where coverage from only one radar (Monte Lema) is available.

[56] Taking into account that both the stochastic models used in this study are stationary in space and time, various problems in their application can occur if the orographic effects in the study area are strong. As shown in Figure 2b, due to the relatively small extent of the study area, precipitation can be considered as approximately homogeneous. Moreover, in order to take into account the spatial heterogeneity of precipitation, detailed knowledge of the spatial distribution of cumulated precipitation is needed, at least for the calibration of STREAP. Due to the radar measurement errors described above, we chose to use the spatially homogeneous version of the model, which we believe is adequate to serve as a proof-of-concept of the STREAP model capabilities.

7. Results and Discussion

[57] A stochastic model should reproduce rainfall statistics for a wide range of spatial and temporal scales, not only for those that have been used in model calibration. In this study, we validate the STREAP model on a suite of critical statistics for a range of spatial and temporal aggregation scales that correspond to the most common scales of interest in catchment hydrology. Moreover, we use the NS(s-t) model as a benchmark, in order to reveal what is the added value of the higher complexity of STREAP.

[58] In order to obtain the results presented in this section, realizations of 30 years were simulated for both STREAP and NS(s-t) models. For the NS(s-t) model 50 realizations were simulated, whereas for STREAP only 5, due to the larger computational and memory demands. The simulations of STREAP correspond to the same spatial and temporal resolution as the radar data (2×2 km^2, 5 min). An illustration of the generated precipitation field using STREAP, as well as its parameters for the study area can be found in the online supporting information. The NS(s-t) model is continuous in space and time, so there is no restriction on the temporal and spatial scale of simulation.

7.1. Areal Statistics

[59] The areal statistics for which we validate STREAP and the benchmark NS(s-t) are: (a) the probability distribution of the fraction of wet areas; (b) the probability distribution of the mean areal intensities; (c) the auto/cross correlation of WAR, IMF; and (d) the probability distribution of the duration of wet and dry spells.

7.1.1. WAR and IMF

[60] In order to compare the areal statistics, we used the WAR-IMF series derived for the study region from the radar data. The radar efficiency is considered good and biases are very small for the mean areal rainfall and the fraction of wet area. Deriving WAR-IMF from the station data (11 stations in the study area) is certainly less accurate. However we recognize that this creates a disadvantage for the NS(s-t) model, which was calibrated with station data. For this reason, in the following, we concentrate the NS(s-t) and STREAP comparison only on statistics that should be reasonably represented given the respective data sources for calibration.

[61] The temporal scales for which the model efficiencies are evaluated are 10 min, 1 h, and 1 day. This selection reflects the range of temporal scales of interest both for urban and catchment hydrology. Even though the model calibration is performed on a seasonal basis, only performances for the entire year are presented here. The model efficiency is similar for all of the seasons and thus the overall annual results are representative.

[62] STREAP is very good at reproducing both autocorrelations and the cross correlations of the WAR and IMF processes (Figures 3a–3c). Lower skills can be observed for the autocorrelation of the WAR process at the high-frequency scale (10 min). The underestimation of the autocorrelation at this scale is mostly due to the fact that the model, given the implemented structure of the WAR-IMF process generates abrupt beginnings and ends of storms. However, this problem tends to fade out very rapidly with increasing aggregation scale and is hardly visible at the hourly scale. In contrast, the NS(s-t) model tends not to capture these correlations (Figures 3d–3f).

[63] This result is not surprising since STREAP has been explicitly calibrated to reproduce the correlation statistics. However, what is of major importance is that STREAP performs very well for all the aggregation scales examined, even though it has been calibrated only for one time scale, which in this case is the finest 5 min scale. Another observation is that the simplified approach of the NS(s-t) model is underperforming concerning the joint behavior of the WAR-IMF process. In other words, the NS(s-t) model does not capture storm growth, development and decay in the entire region in a realistic manner.

[64] The observed and simulated probability distributions of IMF and WAR are shown in Figures 4 and 5. The differences between the two models become more apparent for these variables. The STREAP model behaves very well in reproducing both variables for all examined time scales. The NS(s-t) model conversely overestimates both the mean areal intensities and wet area ratios during a storm, compensating with less frequent storms. The reason for this is that the spatial component of the rainfall in the NS(s-t) model is based on the superposition of circular rain cells. Since the size of these cells is independent of their intensity, it may happen that large cells produce very intense precipitation. This behavior is clearly contrasting with reality since very intense precipitation is associated with convective cells that commonly have a small spatial extent. Possibly, in different NS(s-t) models, which have mixtures of rain cells with different statistical properties this problem is mitigated.

7.1.2. Wet Spell Durations

[65] A fundamental property of rainfall for hydrological modeling is the duration of wet spells. The STREAP model is excellent in reproducing wet spells in terms of areal

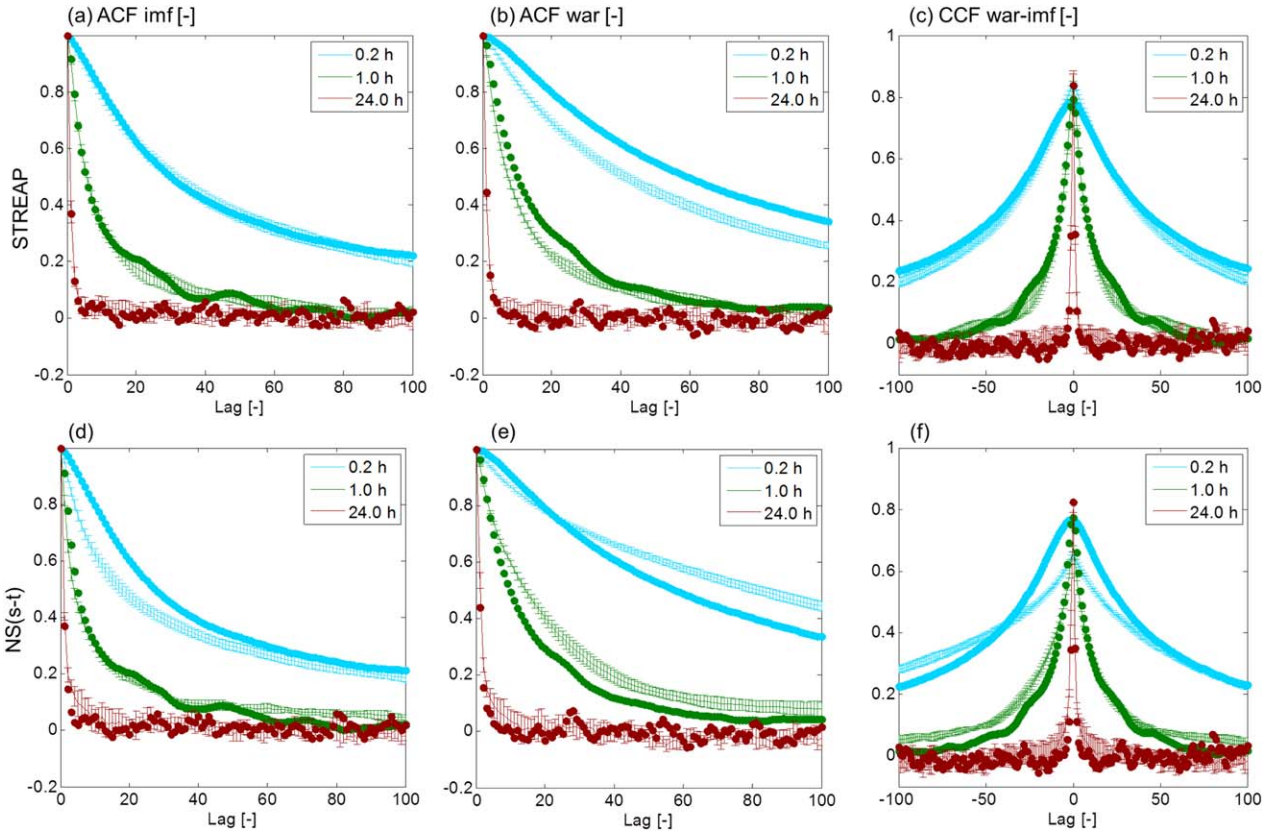

Figure 3. Autocorrelation function of IMF for (a) the STREAP model and (d) the NS(s-t) model. Autocorrelation function of WAR for (b) the STREAP model and (e) the NS(s-t) model. Cross correlation of WAR-IMF for (c) the STREAP model and (f) the NS(s-t) model. Dots correspond to observations and lines to the mean value of an ensemble of simulations. Different colors correspond to different aggregation intervals in the legend. Error bars show the standard deviation from all the realizations. The units of the lag correspond to the respective aggregation scale (e.g., 5 can refer either to 5 days, 5 h, or 5–10 min intervals).

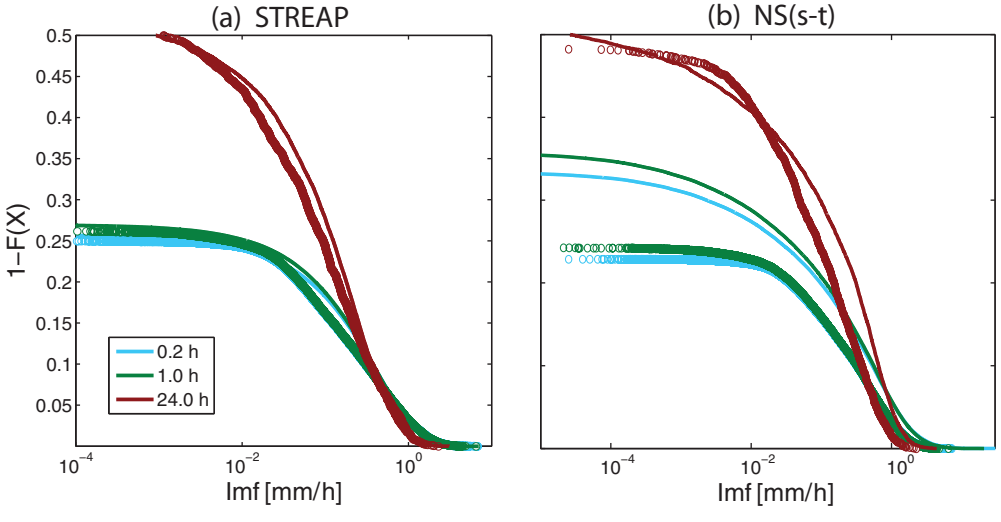

Figure 4. Exceedance probability of the mean areal intensity (a) for the STREAP model and (b) for the NS(s-t) model. Dots correspond to observations and lines to the mean value of an ensemble of simulations. Different colors correspond to different aggregation intervals in the legend.

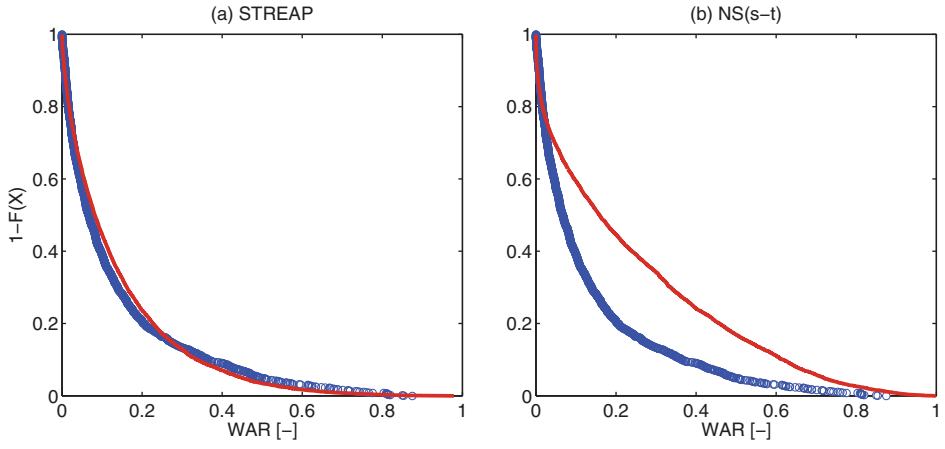

Figure 5. Exceedance probability of the wet area ratio during a storm period (a) for the STREAP model and (b) for the NS(s-t) model. Dots correspond to observations and lines to the mean value of an ensemble of simulations. The results refer to the 10 min time scale.

precipitation, i.e. the duration when a storm occurs at some place in the study area (Figure 6a). A very encouraging result is the consistency of this good behavior across temporal scales. This means that the selected occurrence process for storms at stage 1 of the STREAP model is efficient. On the contrary, the NS(s-t) model performs poorly, showing a tendency toward an underestimation of the wet spell durations for fine temporal scales, and an overestimation for large aggregation scales. This is a clear indication that the Poisson arrival process of the storms in the NS(s-t) is suboptimal.

[66] We illustrate the importance of the spatial distribution of precipitation using another metric introduced by *Bell* [1987]. This metric is the probability distribution of the length of an arbitrary cross section that is covered with precipitation across a radar image and addresses the ability of a model to simultaneously capture the spatial correlation of precipitation, the size of the generated rain cells and the distribution of the wet area ratios. The results evidently show that STREAP can perfectly reproduce the distribution of the length covered with rainfall as estimated from the weather radar dataset (Figure 7). On the contrary, the NS(s-t) model predicts generally much larger areas covered with rainfall. The reason for this is the simulation of very large rain cells that persist in time at a given location.

[67] As a general result, we demonstrate that STREAP provides a detailed and highly satisfactory description of the spatial and temporal component of areal precipitation. The comparison with the simpler NS(s-t) model confirms the added value of STREAP that comes with a much more realistic space-time description of the precipitation process. We acknowledge that the NS(s-t) has been originally developed as a multisite model for rainfall simulation at point locations. Our results show that its use for spatial rainfall simulation results in a simultaneous overestimation of the mean areal rainfall intensities and wet area ratios, and

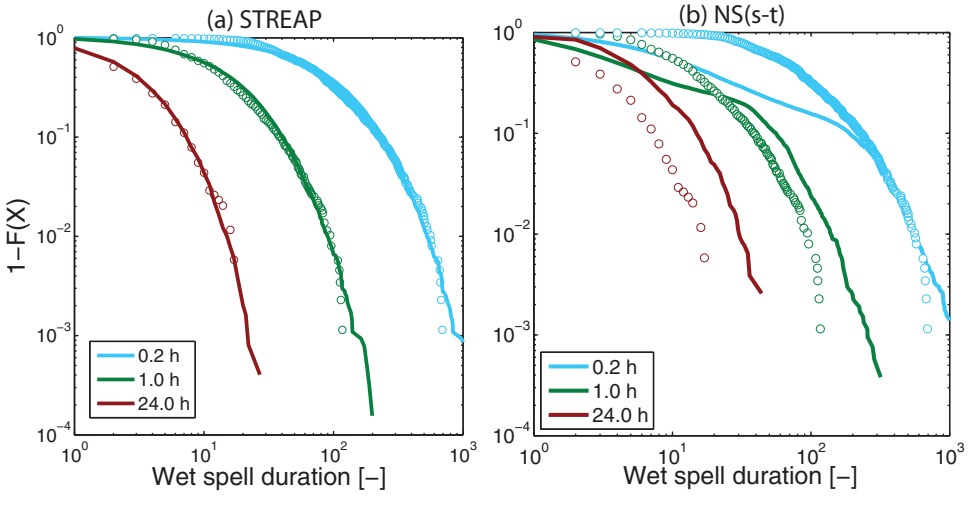

Figure 6. Exceedance probability of the wet spell durations in the study area (a) for the STREAP model and (b) for the NS(s-t) model. Dots correspond to observations and lines to the mean value of an ensemble of simulations. Different colors correspond to different aggregation intervals in the legend. Units of the *x* axis refer to the corresponding scale as in Figure 3.

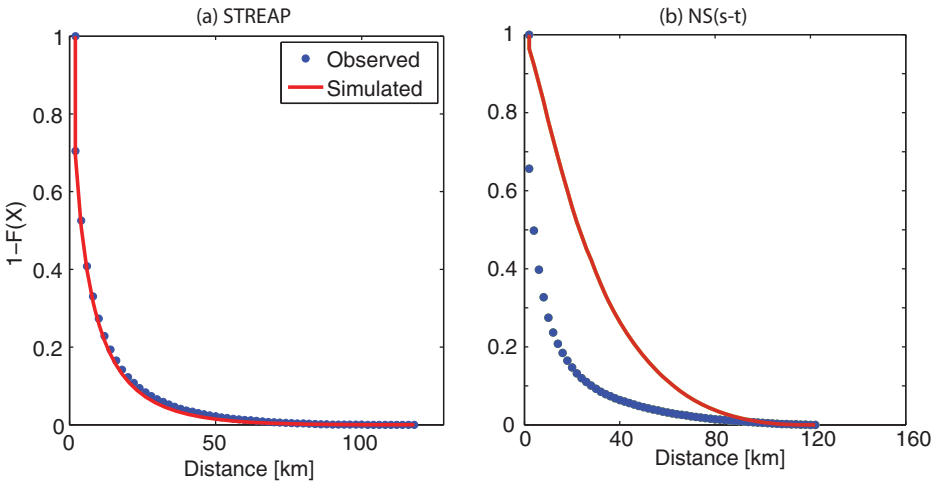

Figure 7. Exceedance probability of the length of an arbitrary cross section covered with rain (a) for the STREAP model and (b) for the NS(s-t) model. Dots correspond to observations and lines to the mean value of an ensemble of simulations.

therefore overall higher rainfall depths for a given storm. Since the model is calibrated to reproduce the point-scale statistics (see next section) this leads to a compensating overestimation of the durations of no rainfall, i.e., the interstorm periods. This can potentially have a major impact, for example, in flood risk analysis, since the total precipitated volume during a storm for the entire area is a crucial factor for flood estimation.

7.2. Point-Scale Statistics

[68] The point statistics for which we validate STREAP represent precipitation properties at the grid cell scale. Unfortunately, a direct comparison of the model output to the rain gauges located in the study area is not possible due to the well-known discrepancies between ground rain gauge measurements and radar precipitation estimates [e.g., *Berne and Krajewski*, 2012]. Since the STREAP model generates homogeneous random fields, a pixel (radar or model) to gauge comparison cannot be made. Therefore, we compare model to radar at the pixel scale. We select at random a number of n pixels ($n \sim 20$) in the study area from the radar image and compute the mean value of the respective statistics. We call this the observed point-scale statistics. Similarly, we take another sample of n pixels from each STREAP simulation and compute their mean, which we call the simulated point-scale statistics that also contains uncertainty that comes from multiple realizations of the space-time model.

[69] For the NS(s-t) model, a direct comparison between model and rain gauges is feasible since NS(s-t) has been explicitly calibrated for reproducing rainfall distributions at the point scale. It should also be noted that an adaptation of the original model [*Burton et al.*, 2008] to take into account the nonhomogeneous precipitation accumulation in space has been adopted. The adaptation consists of a multiplication of the output of the model with a station-dependent scaling factor in order to simultaneously achieve non homogeneity in the precipitation accumulations and good reproduction of precipitation depth for all stations in the study area. For illustrative purposes only the results from the Lugano station are presented here, which is a station with average performance.

[70] In the model comparison, it has to be stressed that the NS(s-t) model has been developed and calibrated to reproduce the point statistics while STREAP was not, which represents the opposite case of the comparison of areal statistics. A good performance of STREAP at the point scale is therefore a robust test of the consistency of the model structure across space and time scales and a good indicator of the general applicability of the model.

7.2.1. Precipitation Depth Distributions

[71] First of all, we examine the probability distributions of precipitation depth for three temporal aggregation intervals (Figure 8). Both models are very good at reproducing the distribution of precipitation at temporal scales larger than 1 h. The major discrepancies for both models occur at the finest temporal scale where both underestimate the tails of the distributions. The underestimation is also dependent on the season. The largest differences occur during the warmer seasons when rainfall is mostly convective and more intense. However, the performance of STREAP equals or even exceeds that of NS(s-t) for these statistics.

[72] The underestimation of the Poisson cluster models for fine temporal scales arises from its structure which simulates rainfall as a superposition of rain cells that cannot introduce variability for temporal and spatial scales less than the average size of the cell (∼1 h, ∼few km). A similar behavior is also seen in the temporal version of the model [*Paschalis*, 2013; *Paschalis et al.*, 2013]. STREAP underestimates the tails of the precipitation distributions mainly because of the choice of using a constant coefficient of variation of spatial rainfall on a monthly basis. However, both models produce reasonably good results for the marginal distributions of precipitation across several temporal scales of hydrological interest.

[73] At longer scales (annual) both models suffer from the well-known overdispersion problem which leads to an underestimation of the interannual variability of precipitation [*Katz and Parlange*, 1998]. If long-term analysis of extremes and interannual variability are of major interest,

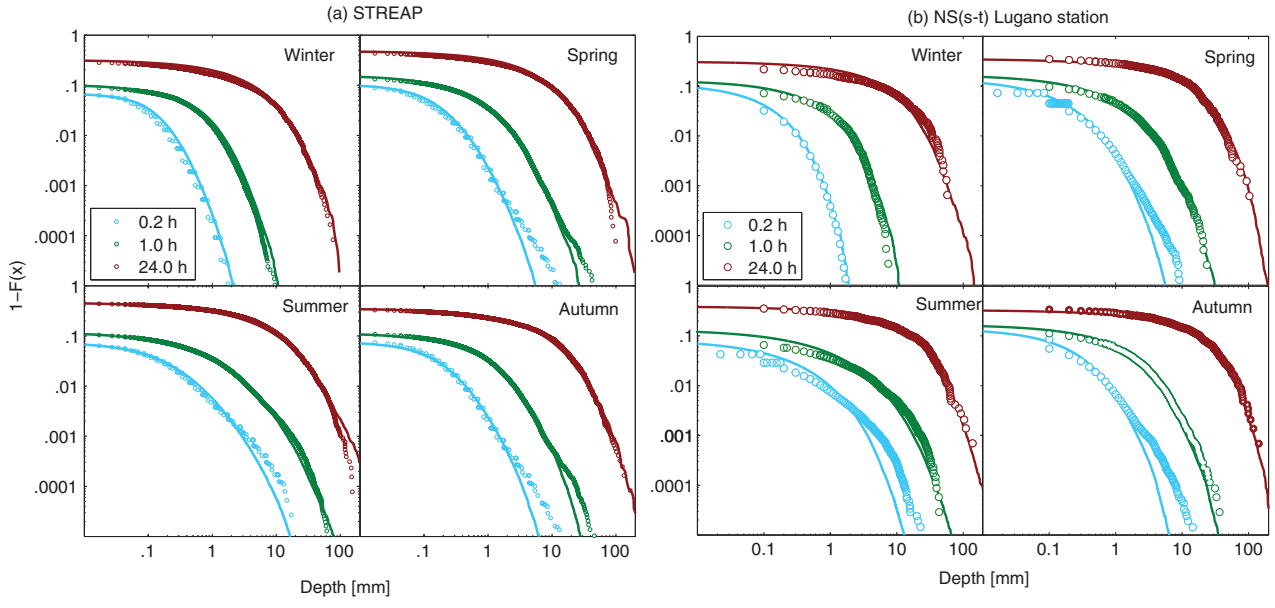

Figure 8. Exceedance probability of the precipitation depth at the point scale (a) for the STREAP model and (b) for the NS(s-t) model for the Lugano station. Dots correspond to observations and lines to simulated series. Different colors correspond to different aggregation intervals in the legend.

modifications of both models are needed [e.g., *Fatichi et al*., 2011].

7.2.2. Intermittency and Wet Spell Duration

[74] Another statistic, the correct reproduction of which is of major interest, is the probability of precipitation occurrence or its complement (intermittency) at the point scale. The STREAP model performs very well in the reproduction of intermittency across scales from minutes to weeks, in contrast to the NS(s-t) model, which systematically overestimates intermittency for large aggregation intervals (Figure 9). This is also a common problem for Poisson cluster models that has been previously addressed in the literature [e.g., *Entekhabi et al*., 1989; *Rodriguez-Iturbe et al*., 1988; *Burlando and Rosso*, 1993; *Onof and Wheater*, 1993; *Paschalis*, 2013]. The success of STREAP is due to the combined effect of capturing the storm arrival process, the temporal evolution of rainy areas, and the spatial autocorrelation of the precipitation process.

[75] The probability distributions of observed and simulated wet spell duration at the point scale are shown in Figure 10. We defined wet spell duration as the period for which precipitation is continuously greater than zero at a

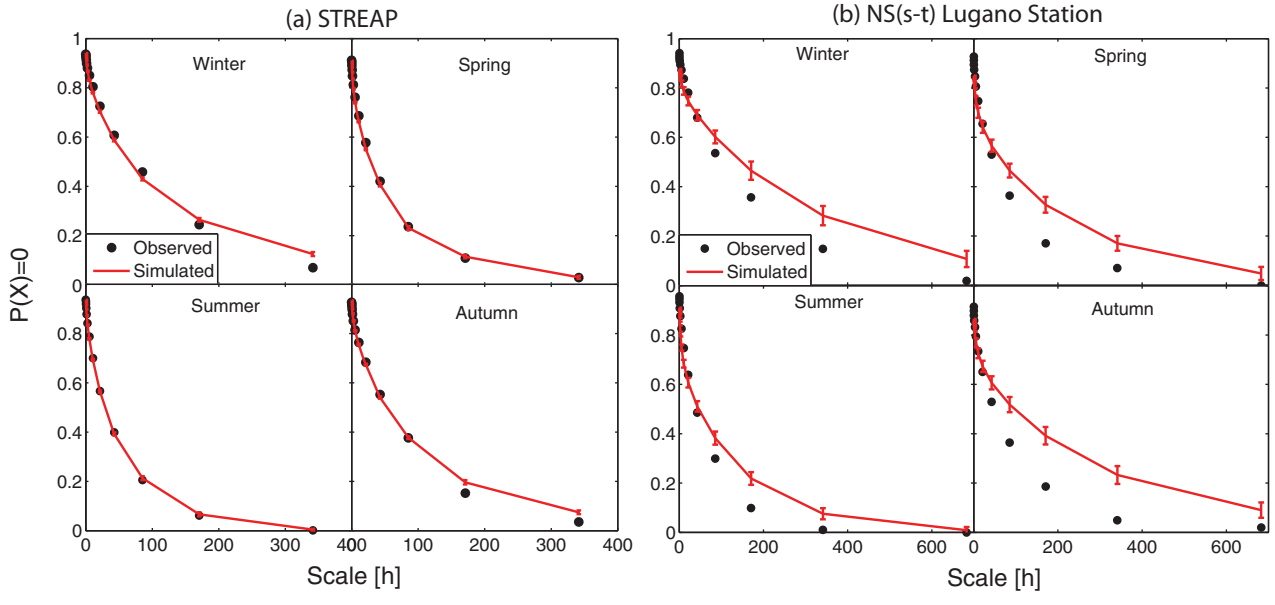

Figure 9. Probability of no precipitation across temporal scales (a) for the STREAP model and (b) for the NS(s-t) model on a seasonal basis. Dots correspond to observations and lines to simulated series. Error bars present the standard deviation of the statistic from simulations.

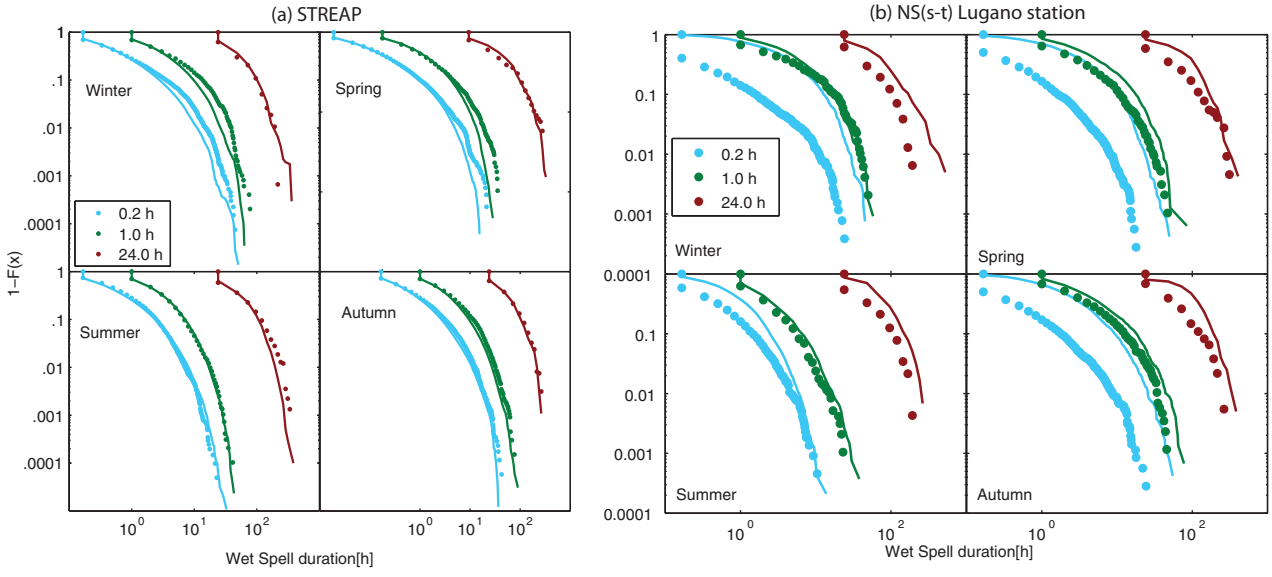

Figure 10. Exceedance probability of the storm (wet spell) duration at the point scale (a) for the STREAP model and (b) for the NS(s-t) model for the Lugano station. Dots correspond to observations and lines to simulations. Different colors correspond to different aggregation intervals in the legend.

pixel scale. Although this is not the conventional way of defining a precipitation event [e.g., *Koutsoyiannis and Foufoula-Georgiou*, 1993], it provides a convenient and consistent definition for the purpose of comparison between observations and simulations. The STREAP model performs well for this statistic for all the examined temporal aggregation scales, except perhaps in the winter and spring when a slight underestimation of long storms is evident. The NS(s-t) model also provides satisfactory results at the daily scale but systematically overestimates the wet spell durations at shorter aggregations. This overestimation is a consequence of the lifetime of the superposed rain cells, which is in the order of hours, thus making very short storms unlikely. In our analysis, the overestimation is also dependent on the season, with summer precipitation being better reproduced.

7.2.3. Autocorrelation

[76] An additional property of point-scale precipitation that is important for hydrological purposes is the persistence of rain at a site. Both models show a similar behavior. The autocorrelation for temporal scales larger than 1 h is reproduced very well, but autocorrelations at the smaller scale are strongly overestimated, except in the winter (Figure 11).

[77] Even though the behavior is similar for both models the reasons of the overestimation at the smaller scales are very different. The overestimation for the NS(s-t) model is due to its inherent incapability of reproducing the small

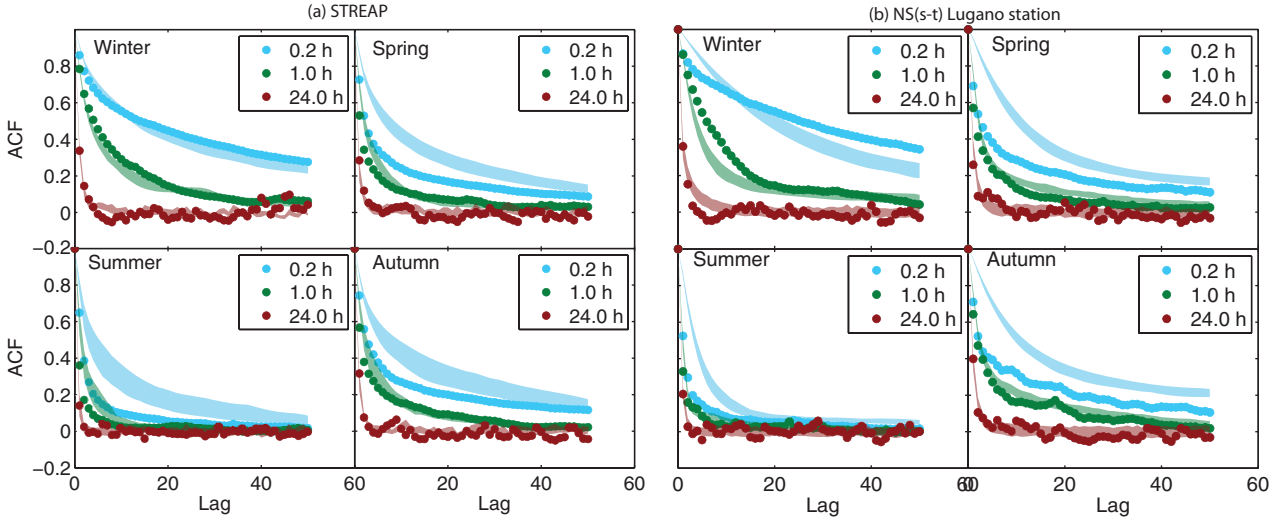

Figure 11. Autocorrelation function of the precipitation depth at the point scale (a) for the STREAP model and (b) for the NS(s-t) model for the Lugano station. Dots correspond to observations and shaded areas to simulations. Different colors correspond to different aggregation intervals in the legend.

temporal-scale variability of rainfall as described before, while the overestimation for STREAP is mainly attributed to the calibration of the ARMA model in the third stage. The conditions we set for the calibration of this process restrict the sample of the storms which are selected for calibration. Restrictions for this selection are a negligible differential movement and rotation, and a long duration. These requirements increase the proportion of winter storms in the selection. This explains the excellent behavior of STREAP for winter precipitation and the largest error during summer, where convective storms are generally localized in space and have short durations and lower autocorrelations.

7.3. Critical Assumptions of STREAP

[78] The model STREAP is developed with two main simplifications: (a) the model assumes homogeneity in space, i.e. the probability of precipitation occurrence and the rainfall accumulation are identical for the entire spatial domain of the simulation; and (b) the simulated rainfall fields are isotropic. The assumption of spatial homogeneity is valid at locations where orographic and microclimatic influences on precipitation are minor. The assumption of rainfall isotropy is based on the extent of the study area. Generally, precipitation fields at the β-mesoscale can be approximated as isotropic [e.g., *Over*, 1995; *Paschalis*, 2013]. Although it has been shown that orographic mechanisms such as blocking of the atmospheric flow can lead to anisotropic patterns in rainfall fields [e.g., *Paschalis*, 2013; *Ebtehaj and Foufoula-Georgiou*, 2010] a stochastic modeling of isotropy can still be a good assumption for many practical applications.

[79] In our study, we chose to adopt these assumptions because to modify STREAP to account for spatial heterogeneity a high accuracy of the distribution of precipitation depth in space is needed. It can be clearly seen in Figure 2c that such information cannot be derived from the current operational weather radar data. Radar measurement errors can seriously affect the observed spatial distribution of precipitation. Specifically, (a) clutter problems can impact the estimation of the probability of precipitation occurrence in given cells, since areas prone to atmospheric clutter corruption report more frequent precipitation; and (b) problems associated with beam shielding and signal attenuation can affect the spatial accumulation of precipitation. As a result adding nonhomogeneity into the model would simply force the model to reproduce errors in precipitation radar data. Nevertheless, the first author has developed an outline of how nonhomogeneity may be included into STREAP provided its structure is known [*Paschalis*, 2013].

8. Conclusions

[80] In this paper, we develop a new stochastic space-time model for precipitation STREAP which reproduces essential features of the statistical structure of precipitation in space and time for a wide range of hydrologically relevant scales (from 10 min to 24 h). The improvements in STREAP are directed at a better reproduction of the basic structural features of precipitation such as intermittency, correlation patterns in space and time, positively skewed probability distribution of intensities, and the growth and decay of storms as they move over the terrain. Following *Pegram and Clothier* [2001b], the model is based on a three stage simulation of (1) the storm arrival process; (2) the process describing the within-storm temporal evolution of areal precipitation properties (wet area ratio WAR and mean intensity IMF); and (3) the process describing the temporal evolution of the two-dimensional storm structure. This model structure has a direct link to the conceptual mechanisms of the precipitation formation processes. We provide the analytical basis for the model and develop its calibration procedure in detail in this paper.

[81] STREAP was calibrated and validated for an area located on the Mediterranean side of the European Alps using 7 years (2004–2010) of high-resolution ($2\times2\text{km}^2$; 5 min) weather radar data. Its performance was compared against a well-known benchmark model, the spatiotemporal version of the Neyman-Scott model (NS(s-t)). Our conclusions arise from a detailed analysis of the efficiency of the two models for both areal and point-scale statistics across a wide range of scales.

[82] In terms of areal statistics, we tested the performance of the models on (a) the probability distribution of the fraction of wet areas; (b) the probability distribution of the mean areal intensities; (c) the auto/cross correlation of WAR, IMF; and (d) the probability distribution of the duration of wet and dry spells. STREAP performs well for all statistics, in particular for the auto/cross correlation of the WAR and IMF processes which the NS(s-t) model fails to capture. A small underestimation in the autocorrelation of the WAR at high resolutions is due to abrupt beginnings and ends of storms in STREAP but this effect disappears rapidly with increasing aggregation scale. Importantly, STREAP performs well for all examined aggregation scales, even though it has been calibrated only for one time scale (5 mins). On the other hand, NS(s-t) overestimates both IMF and WAR during a storm because of the superposition of circular rain cells which have independent size and intensity. The conclusion is that STREAP produces a much more realistic space-time description of the precipitation process which reflects in the areal statistics.

[83] In terms of point statistics, we tested the performance of the models on (a) precipitation depth distributions; (b) intermittency and wet spell duration; and (c) autocorrelation at a point/grid scale. Precipitation depths are satisfactorily reproduced by both models, except perhaps for the tails at high resolution which are underestimated slightly by both models. Intermittency on the other hand is perfectly reproduced by STREAP for all scales, but not by NS(s-t). The success of STREAP is due to the combined effect of capturing the storm arrival process, the temporal evolution of rainy areas, and the spatial autocorrelation of the precipitation process. Autocorrelation is well preserved at coarser resolutions but slightly overestimated at high resolutions. In STREAP, the best performance for autocorrelation is in winter because the model is calibrated on a set of storms which are longer and have negligible differential movement and rotation to get better statistics for storm advection (speed and direction). This biases the success toward winter storms. The conclusion is that STREAP reproduces point statistics as well as the areal statistics even though the model has not been explicitly calibrated to do so. The main result is that STREAP indeed does provide

a more detailed and accurate description of the precipitation process in time and space than the selected popular benchmark model.

[84] Regarding the NS(s-t) model, we found that the good performance of this modeling technique at the point scale (i.e., gauge locations) is associated with a compensation of errors in the spatial representation of rainfall which is inherent in the model structure. The NS(s-t) model, at least in the version we used, cannot capture small-scale variability (subhourly scales) well, thus questioning its utility as rainfall simulator for applications where variability at small spatial and temporal scales is crucial (e.g., urban catchments). Furthermore, being suitable only as a multisite stochastic model, NS(s-t) still requires the use of interpolation techniques for fully distributed applications. It should be noted however that the results refer to the specific tested version of the NS(s-t) model.

[85] STREAP has been developed as a tool for hydrological applications where high-resolution spatiotemporal precipitation is needed, from flood risk simulation for urban catchments and drainage systems, to basin response analysis of large watersheds. The main limitation of the model is in calibration in the sense that good quality high-resolution space-time precipitation data are needed, either from weather radars or dense gauge networks. Although this may limit model applications in parts of the world where data availability is small, it is also true that new developments with remote estimation of rainfall from space will likely provide in the future new data products suitable for calibration [e.g., *Joyce et al*., 2004; *Kummerow et al*., 1998]. This is likely to open a large variety of applications for the STREAP model.

[86] **Acknowledgments.** We would like to thank Geoff Pegram, two anonymous reviewers, and the editor Alberto Montanari for their encouraging comments and their helpful suggestions that improved the manuscript. Precipitation data for Switzerland were provided by MeteoSwiss, the Federal Office of Meteorology and Climatology. Funding for this project was provided by the Swiss National Science Foundation grant 20021–120310.

References

Bárdossy, A., and G. Pegram (2009), Copula based multisite model for daily precipitation simulation, *Hydrol. Earth Syst. Sci.*, *13*, 2299–2314, doi:10.5194/hess-13–2299-2009.

Bell, T. (1987), A space-time stochastic model of rainfall for satellite remote-sensing studies, *J. Geophys. Res.*, *92*(D8), 9631–9643, doi:10.1029/JD092iD08p09631.

Bell, T. and P. K. Kundu (1996), A study of the sampling error in satellite rainfall estimates using optimal averaging of data and a stochastic model, *J. Clim.*, *9*(6), 1251–1268.

Bernardara, P., C. De Michele, and R. Rosso (2007), A simple model of rain in time: An alternating renewal process of wet and dry states with a fractional (non-Gaussian) rain intensity, *Atmos. Res.*, *84*(4), 291–301, doi:10.1016/j.atmosres.2006.09.001.

Berne, A., and W. F. Krajewski (2012), Radar for hydrology: Unfulfilled promise or unrecognized potential?, *Adv. Water Resour.*, *51*, 357–366, doi:10.1016/j.advwatres.2012.05.005.

Beuchat, X., B. Schaefli, M. Soutter, and A. Mermoud (2011), Toward a robust method for subdaily rainfall downscaling from daily data, *Water Resour. Res.*, *47*, W09524, doi:10.1029/2010WR010342.

Bordoy, R. (2013), Spatiotemporal downscaling of climate scenarios in regions of complex orography, PhD thesis, ETH Zurich, Switzerland.

Bougeault, P., P. Binder, A. Buzzi, R. Dirks, J. Kuettner, R. Houze, R. B. Smith, R. Steinacker, and H. Volkert (2001), The MAP special observing period, *Bull. Am. Meteorol. Soc.*, *82*(3), 433–462.

Box, G., and M. Jekins (1970), Time Series Analysis, Forecasting and Control*, Holden-Day*, San Fransisco, Calif.

Bracewell, R. (2000), The Fourier Transform and its Applications, 3rd ed., McGraw-Hill, San Fransisco, Calif.

Brissette, F., M. Khalili, and R. Leconte (2007), Efficient stochastic generation of multi-site synthetic precipitation data, *J. Hydrol.*, *345*(3–4), 121–133, doi:10.1016/j.jhydrol.2007.06.035.

Burlando, P., and R. Rosso (1993), Stochastic models of temporal rainfall: Reproducibility, estimation and prediction of extreme events, in *Stochastic Hydrology in its Use in Water Resources Systems Simulation and Optimization*, Proceedings of NATO-ASI Workshop, edited by J. Salas, R. Harboe, and E. Marco-Segura, pp. 137–173, Kluwer Acad., Peñiscola, Spain.

Burton, A., C. Kilsby, H. Fowler, P. S. Cowpertwait and P. O'Connell (2008), RainSim: A spatial-temporal stochastic rainfall modelling system, *Environ. Modell. Software*, *23*(12), 1356–1369, doi:10.1016/j.envsoft.2008.04.003.

Burton, A., H. J. Fowler, C. G. Kilsby, and P. E. O'Connell (2010), A stochastic model for the spatial-temporal simulation of nonhomogeneous rainfall occurrence and amounts, *Water Resour. Res.*, *46*, W11501, doi:10.1029/2009WR008884.

Buzzi, A., and L. Foschini (2000), Mesoscale meteorological features associated with heavy precipitation in the southern Alpine region, *Meteorol. Atmos. Phys.*, *72*(2–4), 131–146, doi:10.1007/s007030050011.

Chambers, M. (1995), The simulation of random vector time series with given spectrum, *Math. Comput. Modell.*, *22*(2), 1–6.

Chorti, A., and D. Hristopulos (2008), Nonparametric identification of anisotropic (elliptic) correlations in spatially distributed data sets, *IEEE Trans. Signal Process.*, *56*(10), 4738–4751, doi:10.1109/TSP.2008.924144.

Christakos, G. (1987), Stochastic simulation of spatially correlated geoprocesses, *Math. Geol.*, *19*(8), 807–831, doi:10.1007/BF00893018.

Clothier, A. N., and G. G. Pegram (2002), Space-time modelling of rainfall using the string of beads model: Integration of radar and raingauge data, *WRC Tech. Rep. 1010/1/02*, Water Res. Comm., Pretoria.

Cowpertwait, P. S. (2006), A spatial temporal point process model of rainfall for the Thames catchment, UK, *J. Hydrol.*, *330*(3–4), 586–595, doi:10.1016/j.jhydrol.2006.04.043.

Cowpertwait, P. S. (2010), A spatial-temporal point process model with a continuous distribution of storm types, *Water Resour.Res.*, *46*, W12507, doi:10.1029/2010WR009728.

Cowpertwait, P. S., C. Kilsby and P. O'Connell (2002), A space-time Neyman-Scott model of rainfall: Empirical analysis of extremes, *Water Resour. Res.*, *38*(8), 1131, doi:10.1029/2001WR000709.

De Michele, C., and P. Bernardara (2005), Spectral analysis and modeling of space-time rainfall fields, *Atmos. Res.*, *77*(1–4), 124–136, doi:10.1016/j.atmosres.2004.10.031.

De Oliveira, V. (2004), A simple model for spatial rainfall fields, *Stochastic Environ. Res. Risk Assess.*, *18*(2), 131–140, doi:10.1007/s00477-003-0146-4.

Deidda, R. (2000), Rainfall downscaling in a space-time multifractal framework, *Water Resour. Res.*, *36*(7), 1779–1794, doi:10.1029/2000WR900038.

Demarta, S., and A. J. McNeil (2007), The T copula and related copulas, *Int. Stat. Rev.*, *73*(1), 111–129, doi:10.1111/j.1751–5823.2005.tb00254.x.

Durbán, M., and C. Glasbey (2001), Weather modelling using a multivariate latent Gaussian model, *Agric. For. Meteorol.*, *109*(3), 187–201.

Ebtehaj, M., and E. Foufoula-Georgiou (2010), Orographic signature on multiscale statistics of extreme rainfall: A storm-scale study, *J. Geophys. Res.*, *115*, D23112, doi:10.1029/2010JD014093.

Embrechts, P., C. Klüppelberg, and T. Mikosch (1997), *Modelling Extremal Events: For Insurance and Finance*, Springer, New York.

Entekhabi, D., I. Rodriguez-iturbe, and P. S. Eagleson (1989), Probabilistic representation of the temporal rainfall process by a modified Neyman-Scott rectangular pulse model: Parameter estimation and validation, *Water Resour. Res.*, *25*(2), 295–302.

Fatichi, S., V. Y. Ivanov, and E. Caporali (2011), Simulation of future climate scenarios with a weather generator, *Adv. Water Resour.*, *34*(4), 448–467, doi:10.1016/j.advwatres.2010.12.013.

Fatichi, S., V. Y. Ivanov, and E. Caporali (2012a), A mechanistic ecohydrological model to investigate complex interactions in cold and warm water-controlled environments: 1. Theoretical framework and plot-scale analysis, *J. Adv. Model. Earth Syst.*, *4*, M05002, doi:10.1029/2011MS000086.

Fatichi, S., V. Y. Ivanov, and E. Caporali (2012b), A mechanistic ecohydrological model to investigate complex interactions in cold and warm water-controlled environments: 2. Spatiotemporal analyses, *J. Adv. Model. Earth Syst.*, *4*, M05003, doi:10.1029/2011MS000087.

Fatichi, S., S. Rimkus, P. Burlando, R. Bordoy, and P. Molnar (2013), Elevational dependence of climate change impacts on water resources in an Alpine catchment, *Hydrol. Earth Syst. Sci. Discuss.*, *10*(3), 3743–3794, doi:10.5194/hessd-10–3743-2013.

Féral, L., H. Sauvageot, L. Castanet, J. Lemorton, F. Cornet, and K. Leconte (2006), Large-scale modeling of rain fields from a rain cell deterministic model, *Radio Sci.*, *41*(2), 1–21, doi:10.1029/2005RS003312.

Foresti, L., M. Kanevski, and A. Pozdnoukhov (2012), Kernel-based mapping of orographic rainfall enhancement in the Swiss Alps as detected by weather radar, *IEEE Trans. Geosci. Remote Sens.*, *50*(8), 2954–2967, doi:10.1109/TGRS.2011.2179550.

Frei, C., and C. Schär (1998), A precipitation climatology of the Alps from high-resolution rain-gauge observations, *Int. J. Climatol.*, *18*, 873–900, doi:10.1002/(SICI)1097-0088(19980630)18:8<873::AID-JOC255-3.0.CO;2–9.

Germann, U., G. Galli, M. Boscacci, and M. Bolliger (2006), Radar precipitation measurement in a mountainous region, *Q. J. R. Meteorol. Soc.*, *132*(618), 1669–1692, doi:10.1256/qj.05.190.

Gires, A., C. Onof, C. Maksimovic, D. Schertzer, I. Tchiguirinskaia, and N. Simoes (2012), Quantifying the impact of small scale unmeasured rainfall variability on urban runoff through multifractal downscaling: A case study, *J. Hydrol.*, *442*, 117–128, doi:10.1016/j.jhydrol.2012.04.005.

Gneiting, T. (2010), Matérn cross-covariance functions for multivariate random fields, *J. Am. Stat. Assoc.*, *105*(491), 1167–1177, doi:10.1198/jasa.2010.tm09420.

Guillot, G. (1999), Approximation of Sahelian rainfall fields with meta-Gaussian random functions, *Stochastic Environ. Res. Risk Assess.*, *13*(1–2), 100–112, doi:10.1007/s004770050034.

Gutnisky, D. A., and K. Josić (2010), Generation of spatiotemporally correlated spike trains and local field potentials using a multivariate autoregressive process, *J. Neurophysiol.*, *103*(5), 2912–2930, doi:10.1152/jn.00518.2009.

Guttorp, P., and T. Gneiting (2006), Studies in the history of probability and statistics XLIX. On the Matern correlation family, *Biometrika*, *93*(4), 989–995.

Houze, R. A., C. James, and S. Medina (2001), Radar observations of precipitation and airflow on the Mediterranean side of the Alps: Autumn 1998 and 1999, *Q. J. R. Meteorol. Soc.*, *127*(578), 2537–2558, doi:10.1256/smsqj.57803.

Houze, R. J. (2012), Orographic effects on precipitating clouds, *Rev. Geophys.*, *50*, RG1001, doi:10.1029/2011RG000365.

Hristopulos, D., and S. Elogne (2009), Computationally efficient spatial interpolators based on Spartan spatial random fields, *IEEE Trans. Signal Process.*, *57*(9), 3475–3487, doi:10.1109/TSP.2009.2021450.

Hughes, J. P., P. Guttorp, and S. P. Charles (1999), A non-homogeneous hidden Markov model for precipitation occurrence, *J. R. Stat. Soc., Ser. C*, *48*(1), 15–30, doi:10.1111/1467–9876.00136.

Ivanov, V. Y., E. R. Vivoni, R. L. Bras, and D. Entekhabi (2004), Preserving high-resolution surface and rainfall data in operational-scale basin hydrology: A fully-distributed physically-based approach, *J. Hydrol.*, *298*(1–4), 80–111, doi:10.1016/j.jhydrol.2004.03.041.

Joyce, R., J. Janowiak, P. Arkin, and P. Xie (2004), CMORPH: A method that produces global precipitation estimates from passive microwave and infrared data at high spatial and temporal resolution, *J. Hydrometeorol.*, *5*, 487–503.

Kang, B., and J. A. Ramírez (2010), A coupled stochastic space-time intermittent random cascade model for rainfall downscaling, *Water Resour. Res.*, *46*, W10534, doi:10.1029/2008WR007692.

Katz, R., and M. Parlange (1998), Overdispersion phenomenon in stochastic modeling of precipitation, *J. Clim.*, *11*(4), 591–601.

Kleiber, W., R. W. Katz, and B. Rajagopalan (2012), Daily spatiotemporal precipitation simulation using latent and transformed Gaussian processes, *Water Resour. Res.*, *48*, W01523, doi:10.1029/2011WR011105.

Kollet, S. J., and R. M. Maxwell (2008), Capturing the influence of groundwater dynamics on land surface processes using an integrated, distributed watershed model, *Water Resour. Res.*, *44*, W02402, doi:10.1029/2007WR006004.

Koutsoyiannis, D. (2011), Scale of water resources development and sustainability: Small is beautiful, large is great, *Hydrol. Sci. J.*, *56*(4), 553–575, doi:10.1080/02626667.2011.579076.

Koutsoyiannis, D., and E. Foufoula-Georgiou (1993), A scaling model of a storm hyetograph, *Water Resour.*, *29*(7), 2345–2361, doi:10.1029/93WR00395.

Koutsoyiannis, D., A. Paschalis, and N. Theodoratos (2011), Two-dimensional Hurst-Kolmogorov process and its application to rainfall fields, *J. Hydrol.*, *398*(1–2), 91–100, doi:10.1016/j.jhydrol.2010.12.012.

Kumar, P., and T. Bell (2006), Space-time scaling behavior of rain statistics in a stochastic fractional diffusion model, *J. Hydrol.*, *322*(1–4), 49–58, doi:10.1016/j.jhydrol.2005.02.031.

Kummerow, C., W. Barnes, T. Kozu, J. Shiue, and J. Simpson (1998), The tropical rainfall measuring mission (TRMM) sensor package, *J. Atmos. Oceanic Technol.*, *15*(3), 809–817, doi:10.1175/1520-0426(1998)015<0809:TTRMMT>2.0.CO;2.

Kundu, P. K., and T. Bell (2003), A stochastic model of space-time variability of mesoscale rainfall: Statistics of spatial averages, *Water Resour. Res.*, *39*(12), 1328, doi:10.1029/2002WR001802.

Lakshmanan, V., R. Rabin, and V. DeBrunner (2003), Multiscale storm identification and forecast, *Atmos. Res.*, *67–68*, 367–380, doi:10.1016/S0169–8095(03)00068-1.

Lang, A., and J. Potthoff (2011), Fast simulation of Gaussian random fields, *Monte Carlo Methods Appl.*, *17*(3), 195–214.

Leonard, M., M. Lambert, A. Metcalfe, and P. S. Cowpertwait (2008), A space-time Neyman Scott rainfall model with defined storm extent, *Water Resour. Res.*, *44*, W09402, doi:10.1029/2007WR006110.

Li, L., W. Schmid, and J. Joss (1995), Nowcasting of motion and growth of precipitation with radar over a complex orography, *J. Appl. Meteorol.*, *34*(6), 1286–1300, doi:10.1175/1520-0450(1995)034¡1286:NOMAGO¿2.0.CO;2.

Mandapaka, P. V., W. F. Krajewski, R. Mantilla, and V. K. Gupta (2009), Dissecting the effect of rainfall variability on the statistical structure of peak flows, *Adv. Water Resour.*, *32*(10), 1508–1525, doi:10.1016/j.advwatres.2009.07.005.

Mellor, D. (1996), The modified turning bands (MTB) model for space-time rainfall. I. Model definition and properties, *J. Hydrol.*, *175*, 113–127.

Mellor, D. and P. O'Connell (1996), The modified turning bands (MTB) model for space-time rainfall. II. Estimation of raincell parameters, *J. Hydrol.*, *175*(1–4), 129–159, doi:10.1016/S0022–1694(96)80008-4.

Menabde, M., and M. Sivapalan (2000), Modeling of rainfall time series and extremes using bounded random cascades and Levy-stable distributions, *Water Resour. Res.*, *36*(11), 3293–3300, doi:10.1029/2000WR900197.

Menabde, M., A. Seed, D. Harris, and G. Austin (1997), Self-similar random fields and rainfall simulation, *J. Geophys. Res.*, *102*(D12), 509–515, doi:10.1029/97JD00915.

Molnar, P., and P. Burlando (2008), Variability in the scale properties of high-resolution precipitation data in the Alpine climate of Switzerland, *Water Resour. Res.*, *44*, W10404, doi:10.1029/2007WR006142.

Montanari, A., and D. Koutsoyiannis (2012), A blueprint for process-based modeling of uncertain hydrological systems, *Water Resour. Res.*, *48*, W09555, doi:10.1029/2011WR011412.

Ng, W., and U. Panu (2010), Comparisons of traditional and novel stochastic models for the generation of daily precipitation occurrences, *J. Hydrol.*, *380*, 222–236, doi:10.1016/j.jhydrol.2009.11.002.

Onof, C., and H. S. Wheater (1993), Modelling of British rainfall using a random parameter Bartlett-Lewis rectangular pulse model, *J. Hydrol.*, *149*(1–4), 67–95, doi:10.1016/0022–1694(93)90100-N.

Over, T. M. (1995), Modeling space-time rainfall at the mesoscale using random cascades, PhD thesis, Univ. of Colo., Boulder.

Over, T. M. and V. K. Gupta (1996), A space-time theory of mesoscale rainfall using random cascades, *J. Geophys. Res.*, *101*(D21), 26,319–26,331, doi:10.1029/96JD02033.

Panziera, L., and U. Germann (2010), The relation between airflow and orographic precipitation on the southern side of the Alps as revealed by weather radar, *Q. J. R. Meteorol. Soc.*, *136*(646), 222–238, doi:10.1002/qj.544.

Papoulis, A., and S. Unnikrishna (2002), *Probability, Random Variables and Stochastic Processes*, 4th ed., McGraw-Hill, New York.

Paschalis, A. (2013), Modelling the space time structure of precipitation and its impact on basin response, PhD thesis, ETH Zurich, Switzerland.

Paschalis, A., P. Molnar and P. Burlando (2012), Temporal dependence structure in weights in a multiplicative cascade model for precipitation, *Water Resour. Res.*, *48*, W01501, doi:10.1029/2011WR010679.

Paschalis, A., P. Molnar, S. Fatichi, P. Burlando (2013), On temporal stochastic modeling of precipitation, nesting models across scales, *Advances in Water Resources*, in press.

Pathirana, A., and S. Herath (2002), Multifractal modelling and simulation of rain fields exhibiting spatial heterogeneity, *Hydrol. Earth Syst. Sci.*, *6*(4), 659–708.

Pecknold, S., S. Lovejoy, D. Schertzer, C. Hooge, and J. Malouin (1993), The simulation of universal multifractals, in *Cellular Automata*, vol. 1, edited by J. M. Perdgang and A. Lejeune, pp. 228–267, World Scientific, River Edge, N. J.

Pegram, G. G., and A. N. Clothier (2001a), High resolution space-time modelling of rainfall: The ''String of Beads'' model, *J. Hydrol.*, *241*, 26–41, doi:10.1016/S0022–1694(00)00373-5.

Pegram, G. G., and A. N. Clothier (2001b), Downscaling rainfields in space and time, using the String of Beads model in time series mode, *Hydrol. Earth Syst. Sci.*, *5*(2), 175–186, doi:10.5194/hess-5–175-2001.

Rigon, R., G. Bertoldi, and T. M. Over (2006), GEOtop: A distributed hydrological model with coupled water and energy budgets, *J. Hydrometeorol.*, *7*(3), 371–388, doi:10.1175/JHM497.1.

Rinehart, R., and E. Garvey (1978), Three-dimensional storm motion detection by conventional weather radar, *Nature*, *273*, 287–289, doi:10.1038/273287a0.

Rodriguez-Iturbe, I., D. R. Cox, and V. Isham (1988), A point process model for rainfall: Further developments, *Proc. R. Soc. London, Ser. A*, *417*(1853), 283–298, doi:10.1098/rspa.1988.0061.

Roldan, J., and D. A. Woolhiser (1982), Stochastic daily precipitation models. 1. A comparison of occurrence processes, *Water Resour. Res.*, *18*(5), 1451–1459.

Rotunno, R., and R. Houze (2007), Lessons on orographic precipitation from the Mesoscale Alpine Programme, *Q. J. R. Meteorol. Soc.*, *133*(625), 811–830, doi:10.1002/qj.

Savina, M., B. Schäppi, P. Molnar, P. Burlando, and B. Sevruk (2012), Comparison of a tipping-bucket and electronic weighing precipitation gage for snowfall, *Atmos. Res.*, *103*, 45–51, doi:10.1016/j.atmosres.2011.06.010.

Schertzer, D., and S. Lovejoy (1987), Physical modeling and analysis of rain and clouds by anisotropic scaling multiplicative processes, *J. Geophys. Res.*, *92*(D8), 9693–9714, doi:10.1029/JD092iD08p09693.

Schleiss, M., J. Jaffrain, and A. Berne (2012), Stochastic simulation of intermittent DSD fields in time, *J. Hydrometeorol.*, *13*(2), 621–637, doi:10.1175/JHM-D-11–018.1.

Storvik, G., A. Frigessi, and D. Hirst (2002), Stationary spacetime Gaussian fields and their time autoregressive representation, *Stat. Modell.*, *2*(2), 139–161, doi:10.1191/1471082x02st029oa.

Veneziano, D. (2002), Iterated random pulse processes and their spectral properties, *Fractals*, *10*(1), 1–11, doi:10.1142/S0218348X02000884.

Veneziano, D., and C. Lepore (2012), The scaling of temporal rainfall, *Water Resour. Res.*, *48*, W08516, doi:10.1029/2012WR012105.

Waymire, E., V. K. Gupta, and I. Rodriguez-Iturbe (1984), A spectral theory for rainfall intensity at meso-beta scale, *Water Resour. Res.*, *20*(10), 1453–1465, doi:10.1029/WR020i010p01453.

Wilks, D. (1998), Multisite generalization of a daily stochastic precipitation generation model, *J. Hydrol.*, *210*(1–4), 178–191, doi:10.1016/S0022–1694(98)00186-3.

Wilks, D. (1999), Simultaneous stochastic simulation of daily precipitation, temperature and solar radiation at multiple sites in complex terrain, *Agric. For. Meteorol.*, *96*(1–3), 85–101, doi:10.1016/S0168–1923(99)00037-4.